ANNUAL REVIEWS

Annual Review of Materials Research

Materials for Automotive Lightweighting

Alan Taub,[1,2] Emmanuel De Moor,[3] Alan Luo,[4] David K. Matlock,[3] John G. Speer,[3] and Uday Vaidya[5,6,7]

[1]Departments of Materials Science & Engineering and Mechanical Engineering, University of Michigan, Ann Arbor, Michigan 48109, USA; email: alantaub@umich.edu

[2]Lightweight Innovations for Tomorrow (LIFT), Detroit, Michigan 48216, USA; email: ataub@lift.technology

[3]George S. Ansell Department of Metallurgical and Materials Engineering and Advanced Steel Processing and Products Research Center, Colorado School of Mines, Golden, Colorado 80401, USA

[4]Departments of Materials Science & Engineering and Integrated Systems Engineering, The Ohio State University, Columbus, Ohio 43210, USA

[5]Department of Mechanical, Aerospace and Biomedical Engineering, University of Tennessee, Knoxville, Tennessee 37996, USA

[6]Institute for Advanced Composites Manufacturing Innovation (IACMI), Knoxville, Tennessee 37932, USA

[7]Manufacturing Demonstration Facility, Oak Ridge National Laboratory, Knoxville, Tennessee 37932, USA

Annu. Rev. Mater. Res. 2019. 49:327–59

The *Annual Review of Materials Research* is online at matsci.annualreviews.org

https://doi.org/10.1146/annurev-matsci-070218-010134

Keywords

advanced high-strength steel, aluminum, magnesium, polymer composites, lightweighting, multimaterial joining

Abstract

Reducing the weight of automobiles is a major contributor to increased fuel economy. The baseline materials for vehicle construction, low-carbon steel and cast iron, are being replaced by materials with higher specific strength and stiffness: advanced high-strength steels, aluminum, magnesium, and polymer composites. The key challenge is to reduce the cost of manufacturing structures with these new materials. Maximizing the weight reduction requires optimized designs utilizing multimaterials in various forms. This use of mixed materials presents additional challenges in joining and preventing galvanic corrosion.

INTRODUCTION

Reducing the weight of the machines that move people and goods is a key enabler for improving fuel economy and payload (1, 2). The value of weight reduction depends on the particular mode of transportation. **Table 1** compares the financial benefits of reduced weight for both light vehicles and heavy trucks. For light vehicles, weight reduction improves fuel economy at equivalent levels of acceleration. A good rule of thumb for today's automobiles is that a 10% weight reduction delivers a 6% fuel economy improvement (3). For the new battery electric vehicles, it is necessary to offset the increased weight of the propulsion system that results from the lower energy density of batteries relative to liquid fuels (4). Reducing the vehicle weight even further can increase the driving range of these vehicles, yielding an approximately 14% improvement in electric range for a 10% reduction in weight (5). Managing vehicle weight also enables better handling at a 50:50 weight balance. For US operators of class 8 tractor-trailers, the cost of diesel fuel exceeds the cost of the driver, accounting for approximately 40% of operating costs (2). For more than 80% of trips, the trailer is volume constrained, so the benefit of weight reduction is increased fuel economy. These vehicles can achieve an ~0.5% fuel efficiency improvement for every 2,000 kg in weight reduction (2). The trend toward denser freight is leading to increased weight-limited transport. In those cases, reducing weight enables higher payload. The key metric is how much freight can be moved for the least fuel consumption.

The Corporate Average Fuel Economy (CAFE) regulations were enacted in 1975 in reaction to the 1973–1974 oil embargo. Those standards required improved fuel economy of cars and light trucks, leading to an era of decreased vehicle weight of the US fleet (6–8). From 1985 to 2000, vehicle weight increased due to the additional vehicle content needed to meet regulations and consumer requirements (**Figure 1**). Starting around 2005, the weight of vehicles leveled off as further improvements in weight reduction technology were utilized to offset further increases in content (9–11). During this era, despite no improvement in weight, the fuel economy increased as a result of improved powertrain efficiency.

Today's newer models have significantly lower weight than the vehicles they are replacing (12). The new platform 2012 Cadillac ATS sedan weighs 1,504 kg, making it one of the lightest vehicles in its class, due to an all-aluminum hood, magnesium engine mounts, and other lightweight materials (8). Building on the learnings of the aluminum-intensive Jaguar, Ford implemented an aluminum-intensive architecture for the Ford F-150, the bestselling vehicle in North America. The aluminum body, together with an advanced high-strength steel frame, resulted in a weight reduction of more than 300 kg (a 14% decrease) compared to the model year 2014 vehicle (13–16).

WEIGHT REDUCTION BY OPTIMIZED DESIGN

Weight reduction can be accomplished by minimizing the amount of material needed to support the structural loads. Advances in design methods, such as topology optimization, can lead to reduced weight components, delivering equivalent mechanical performance (17). Topology optimization tools are now readily available in commercial software for use by design engineers. For example, optimizing the location bolt holes in an engine block reduced weight by more than 30%

Table 1 Financial benefits of reducing weight

Sector	Value of weight reduction ($/kg)	Reference
Light vehicle	$4.50/kg	1
Heavy truck	$5–11/kg dry van dedicated routes	2
Heavy truck	$13–24/kg bulk carriers	2

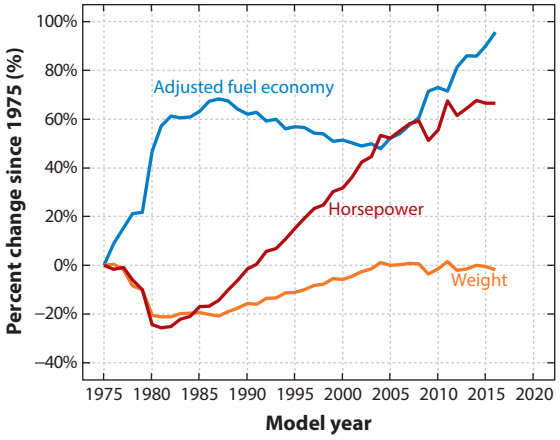

Figure 1

Changes in adjusted fuel economy, weight, and horsepower for model years 1975–2016. Adapted with permission from Reference 11.

and reduced the weight of an aluminum extrusion clamp by 14% (18). Significantly, these design changes can often be implemented with no impact on cost. Further weight reductions can be achieved by combining optimized design with improved manufacturing capability. Tailor-welded blanks provide additional capability to optimize the gauge of sheet metal while maintaining large integral stampings. Use of thinner wall ductile iron castings combined with design optimization can deliver as much as a 40% weight reduction (19).

The next-generation design optimization methodology based on integrated computational materials engineering (ICME) will lead to further weight reduction opportunities (20, 21). The ICME models of both the material and the manufacturing process bridge the dimensional scales from the atomistic level to the component level. The models can simulate the temperature and strain history, as well as the microstructure evolution in each section of the material as it is being processed. The final microstructure can then be predicted with its associated mechanical properties. The ICME models can allow for modifications of the processing conditions for optimal microstructure evolution. The ICME tools were first applied to castings and are now being extended to thermomechanical and powder processing. As a result, virtual components can now be designed, processed, and tested for durability on a workstation long before components are fabricated (22). The future vision for weight reduction by ICME modeling is to enable the engineer to design components using local properties as determined from the model. In contrast, today's methodology employs average properties across the entire component. Further improvements can be envisioned when the ICME tools are developed to the level at which they can be integrated with topology optimization software.

The processes that are used to manufacture components can generally be grouped into the broad categories of casting, thermomechanical processing, and powder consolidation for metals and various thermo-forming approaches for polymer composites. Casting and thermomechanical processing of metals have been practiced for thousands of years. Powder metallurgy and polymer composite processing are more recent developments. As mass customization has become more common, agile processes requiring low capital investment have emerged; such processes include additive manufacturing (23) and incremental sheet forming (24–27) (**Figure 2**). Additive manufacturing not only is cost effective for low-volume production but also allows for production of components with higher geometrical complexity. This capability allows for further

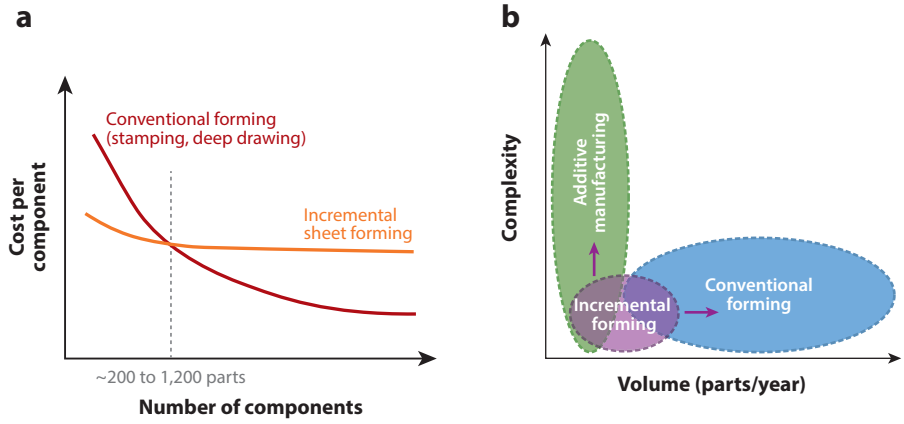

Figure 2

(*a*) Incremental forming and cost-effectiveness at low volume production relative to traditional forming technologies. (*b*) Balance of part complexity and production volume for different forming processes.

weight reduction by enabling true topology-optimized structures that cannot be formed by more conventional processes.

WEIGHT REDUCTION BY MATERIAL SUBSTITUTION

Weight reduction is possible through the use of materials having either higher specific stiffness or strength, depending on the load path. Many studies of light vehicles have demonstrated the potential for weight savings by material substitution (28). For the body structure, weight savings as high as 60% can be obtained (**Table 2**). However, weight reduction comes with a significant cost penalty. For applications that involve common materials as opposed to expensive rare elements, increased costs can be related to the costs of energy and the processes that are used to refine and manufacture the raw materials into the desired component shapes.

At the beginning of the automotive industry, several materials were evaluated as substitutes for wood in the car, including low-carbon steels, aluminum, and bio-based polymers (3, 29). Steel soon became the dominant material due to its low cost, the ability to stamp the sheet at ambient temperature, and its robust spot weldability. Toward the end of the last century, there were many investigations for replacing steel as the main material for the body structure, and a number of aluminum-intensive and polymer composite–intensive vehicle prototypes with significant weight savings were reported. Today, the focus has moved from single-material-intensive body structures to designs using multimaterials (steel, aluminum, magnesium, and polymer composites)

Table 2 Impact of material substitution (5)

Lightweight material	Material replaced	Mass reduction (%)	Relative cost per part
Magnesium	Mild steel, cast iron	60–75	1.5 to 2.5
Carbon fiber composites	Mild steel	50–60	2 to 10+
Aluminum metal matrix composites	Mild steel, cast iron	40–60	1.5 to 3+
Aluminum	Mild steel, cast iron	40–60	1.3 to 2
Titanium	Mild steel	40–55	1.5 to 10+
Glass fiber composites	Mild steel	25–35	1 to 1.5
Advanced high-strength steel	Mild steel	15–25	1 to 1.5

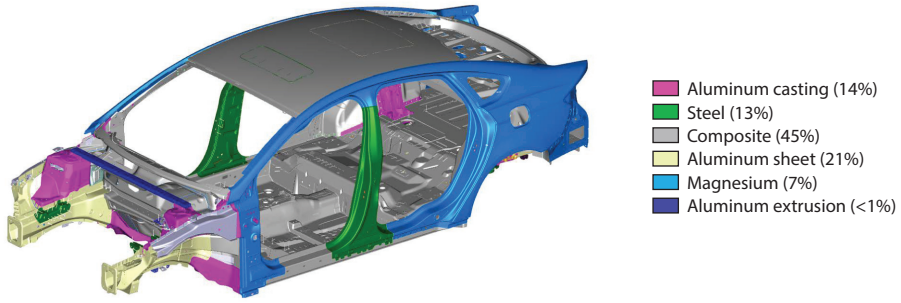

Figure 3

Mixed-material lightweight vehicle Mach-II body-in-white material distribution. Adapted from Reference 30.

manufactured in multiple forms (sheets, extrusions, and castings) (30–34) (**Figure 3**). Designs now use the right material in the right form for each structural subsystem (35–41). The challenge for utilizing these lighter-weight materials is to develop new manufacturing processes for mixed-material structures that meet the cost requirements for the particular application. This use of mixed materials also presents additional challenges in joining and preventing galvanic corrosion (42–44).

Steel and aluminum are the major materials used in structural applications, with the industry also seeing increased use of magnesium and polymer composite components (**Figure 4**). This article reviews advances that are being made in these material systems. The discussion focuses mainly on body, chassis, and interior components. The increasing trend toward partial and full electrification of the powertrain offers additional opportunities that are beyond the scope of this review.

FERROUS ALLOYS: ADVANCED HIGH-STRENGTH STEELS AND DUCTILE CAST IRON

Historically, automobiles have contained significant amounts of ferrous alloys, as both wrought steels and cast irons. Ferrous alloy and product developments, which have led to higher-strength

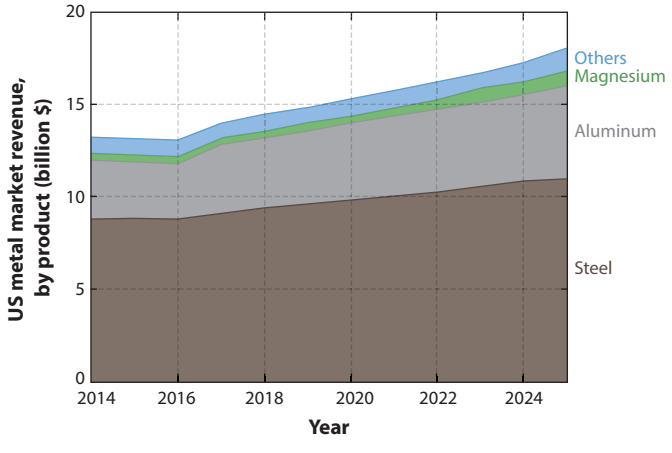

Figure 4

US automotive metal market history and projection. Adapted from Reference 28.

materials with significantly enhanced properties, have been instrumental in enabling economic lightweight solutions in vehicles, including lighter-weight structural components for the critical safety cage, such as the body in white, thinner sheet steel for exposed panels, and higher-power-density transmissions and driveline components. Examples of enhanced properties of interest are total elongation or ductility, formability, the ability to absorb energy in crash situations, corrosion resistance, weldability, fatigue resistance, and fracture toughness. The improvements have been achieved, and are continuing to be achieved, by alloy and process modifications leading to cleaner steels with significantly reduced inclusion contents, lower amounts of residual elements, and the desired microstructures. Thin-wall casting procedures have resulted in more microstructurally homogeneous products with minimal defects and undesirable constituents, both of which are often present in conventional castings. In this section, three ferrous alloy systems—advanced sheet steels, bar and forging steels, and thin-wall austempered ductile iron (ADI) castings—are assessed to illustrate how unique combinations of strength increases and enhanced properties are achieved to improve performance in lightweight designs.

Advanced High-Strength Sheet Steels

First-generation advanced high-strength sheet steels (AHSS)—which include dual-phase (DP), complex-phase, transformation-induced plasticity (TRIP), and martensitic steels—have been developed and are currently being employed for cold-formed parts in the production of automobiles. **Figure 5**, a property map in ultimate tensile strength–total tensile elongation space, shows that the first-generation AHSS exhibit superior strength/elongation combinations in comparison to many steels, including conventional low-strength grades (e.g., interstitial free, bake hardened, and carbon-manganese mild steels) and conventional higher-strength grades (e.g., high-strength low-alloy and ferritic bainitic steels) (45). Typically, higher-ductility steels exhibit better formability, and thus the data in **Figure 5** provide a comparative guide for assessing potential formability. **Figure 5** also shows that alloying and processing strategies that lead to austenitic stainless steels and twinning-induced plasticity (TWIP) steels result in steels at specific strength levels with total elongations significantly greater than those of first-generation AHSS. However, such steels, referred to as second-generation AHSS, are expensive due to high alloy additions and have not

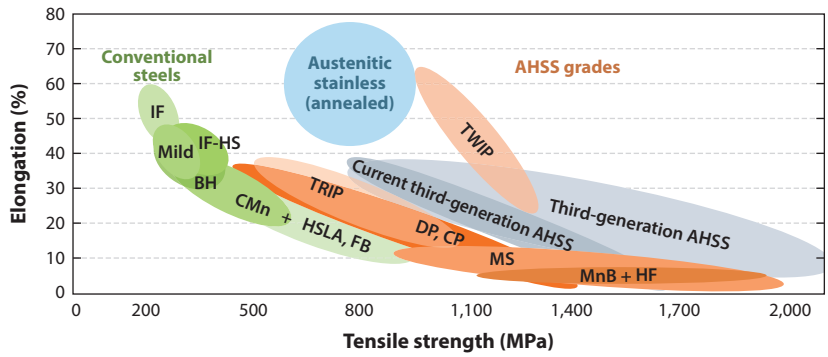

Figure 5

A property map of tensile strength and total elongation combinations for various classes of conventional and AHSS grades. Abbreviations: AHSS, advanced high-strength sheet steel; BH, bake hardened; CP, complex phase; DP, dual phase; FB, ferritic bainitic; HF, hot formed; HSLA, high strength low alloy; IF, interstitial free; IF-HS, interstitial free–high strength; MS, martensitic; TRIP, transformation-induced plasticity; TWIP, twinning-induced plasticity. Adapted with permission from Reference 45.

been extensively incorporated into the manufacture of automobiles. While the data presented in **Figure 5** were obtained under quasi-static testing conditions, similar comparisons, albeit at different strength/elongation combinations, would be observed for data obtained at the high strain rates characteristic of actual stamping operations or crash events.

Extensive research and product development efforts have concentrated on producing cost-effective steels with tensile properties within the two adjacent bands identified as third-generation AHSS (46, 47). Deformation models have shown that steels with third-generation AHSS properties require complex microstructures consisting of high-strength constituents (e.g., martensite, bainite, or ultrafine-grained ferrite) and significant amounts of retained austenite with controlled stability against transformation to martensite with strain (47, 48). During deformation, the retained austenite can transform to martensite, increasing strength and strain hardening. This process results in necking being delayed to higher strains, i.e., the TRIP effect (49, 50). Multiple alloying and processing strategies have been produced, or are being considered to produce, steels with tensile properties within the third-generation property band (46). Among these strategies are processing to enhance the properties of DP steels; modifications to traditional TRIP steel processing, including TRIP-aided bainitic ferrite steels (51, 52) [a class of TRIP steels referred to as medium-manganese steels with manganese contents between approximately 5 and 12 wt% (53–56)]; modified stainless and TWIP steels with lower levels of expensive alloy additions; and implementation of new processing routes leading to nanostructured bainite (57) or the quenching and partitioning (Q&P) process (58, 59). Novel processing routes for the production of third-generation steels typically use low-alloy steels and derive final microstructures from extension of traditional thermal processing or incorporation of novel thermomechanical strategies. Three economically promising processing approaches for cold-formable steels are considered here, and complete summaries of other approaches are elsewhere (46).

TRIP-aided bainitic ferrite (TBF) steels, a class of steels designed to obtain tensile strengths beyond conventional TRIP steels (51, 52), consist of a matrix of fine bainitic ferrite laths and retained austenite in the absence of intercritical ferrite. TBF steels are produced by heating a conventionally cold-rolled microstructure to a temperature at which the steel is fully austenitic, followed by rapid cooling to an isothermal transformation temperature (referred to as the austempering temperature), typically between 300°C and 500°C (60). A typical composition includes 0.2 wt% C, 1.5 wt% Mn, and 1–2 wt% Si with additions of Cr, Mo, and/or microalloying elements. Typical microstructures consist of bainitic ferrite laths, up to approximately 1 μm in width, interlath-retained austenite up to approximately 16 vol% for higher-carbon TBF alloys (61), and some fresh martensite formed on cooling after austempering. The final microstructures, and thus the mechanical properties, depend on austempering temperature and time. During austempering, austenite is enriched in carbon, which increases the austenite stability (60). **Figure 6** shows a set of tensile curves obtained after austempering at temperatures between 300°C and 500°C (52). All samples exhibit continuous yielding, and the results indicate that the final microstructures vary significantly with temperature and result in tensile properties near the lower border of the third-generation AHSS band shown in **Figure 5**.

Q&P is a thermal processing route designed to obtain steels with microstructures consisting of martensite, potentially some proeutectoid ferrite, and significant amounts of carbon-enriched austenite (58, 59, 62, 63). **Figure 7** is a schematic drawing showing the critical stages in the Q&P process for steel initially heated to form a fully austenitic structure with the austenite carbon content, C_γ, equal to the average bulk carbon content, C_i. Subsequently, the material is rapidly cooled to the quench temperature (QT), selected below the martensite start temperature (M_S), where the initial microstructure includes martensite, the amount determined by the degree of undercooling below M_s, and austenite. Immediately after quenching, the carbon contents of both martensite and

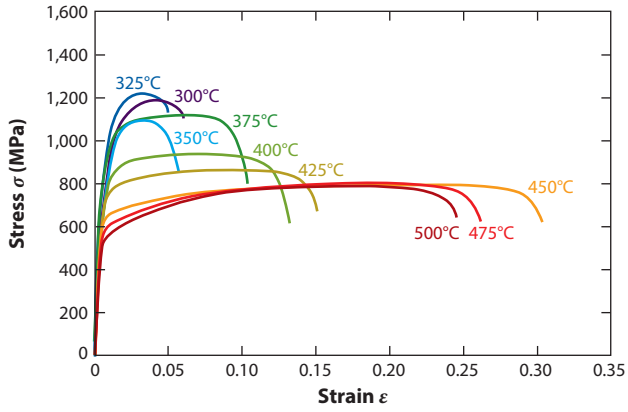

Figure 6

Engineering stress-strain curves of a 0.2 wt% C–1.5 wt% Mn–1.0 wt% Si–0.5 wt% Al steel austempered at varying temperatures ranging between 300°C and 500°C for 200 s. Adapted with permission from Reference 52.

austenite are equal to C_i. Following the quench, the material is held at the partitioning temperature (PT), which is equal either to the QT (one-step Q&P) or, as shown in **Figure 7**, to a higher temperature (two-step Q&P). During the isothermal hold at the PT, carbon partitions from martensite to austenite to increase the austenite stability and to correspondingly decrease the carbon content of the martensite, which may also be undergoing tempering at the PT (64). On cooling to room temperature, some austenite transforms to martensite, and the resulting microstructure consists of carbon-depleted tempered martensite, carbon-enriched metastable austenite, and potentially

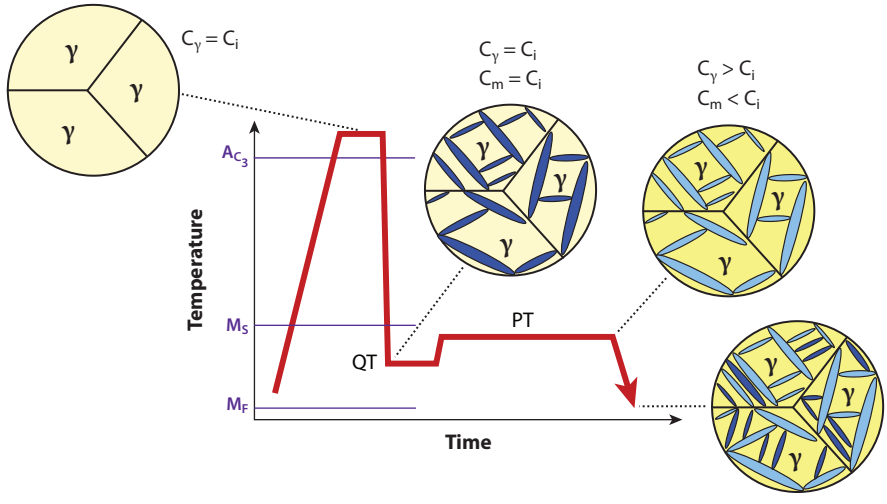

Figure 7

Schematic diagram showing the two-step quenching and partitioning heat treatment process starting with a fully austenitic microstructure. A_{C_3}, M_S, M_F, QT, and PT denote austenitization, martensite start temperature, martensite finish temperature, quenching temperature, and partitioning temperature, respectively. C_i, C_γ, and C_m are carbon contents of the initial alloy, austenite, and martensite, respectively. Adapted with permission from References 46 and 63.

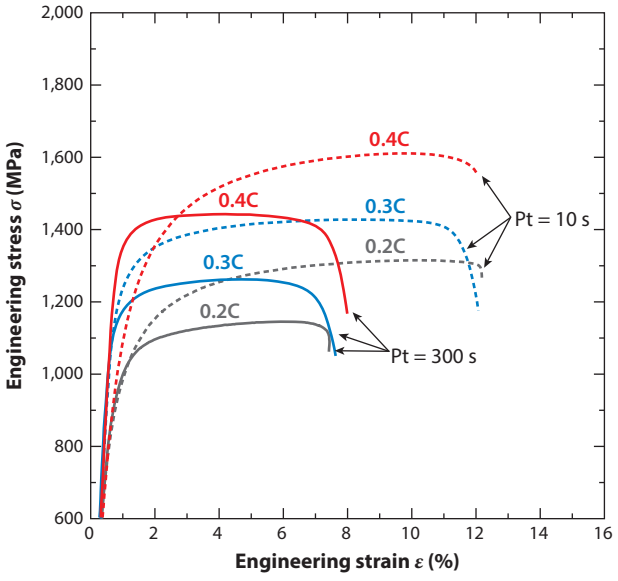

Figure 8

Engineering stress-strain curves obtained in *x* wt% C–1.5 wt% Mn–1.6 wt% Si steels with varying carbon contents from 0.2 to 0.4 wt% after quenching and partitioning processing, with partitioning conducted at 400°C for partitioning times (Pt) of 10 s and 300 s. Adapted with permission from Reference 66.

some untempered martensite formed on final cooling. Steels with austenite volume fractions in the approximate range of 10 to 20 vol% have been produced (58, 59). Models exist to identify the optimal QT (65), and typical Q&P alloys contain C and Mn, with Si added at levels to suppress cementite formation during partitioning (62). The alloys may also include Ni, Cr, and/or Mo. The temperatures and times selected at each stage provide the opportunity to design steels with specific microstructures and thus property combinations, as illustrated in **Figure 8** for steels selected to assess the effects of carbon content and partitioning times (Pt) of 10 s and 300 s (66). **Figure 8** shows that for each Pt, strength increases with carbon content. The samples with Pt of 10 s exhibited higher hardening rates and corresponding significantly higher ductilities than were observed for the samples with Pt of 300 s. As the work hardening rate depends on austenite stability (47), the results in **Figure 8** suggest that retained austenite stability was greater for the samples partitioned for 10 s than for the samples with a Pt of 300 s. Extensive research has shown that the Q&P process is capable of producing high-strength third-generation AHSS products, with the final properties dependent on alloy content and processing history, and initial commercial applications of Q&P steels have been realized (67).

Medium-Mn steels have received considerable recent attention as microstructures with retained austenite volume fractions significantly higher than achievable with TBF or Q&P processing (53–56, 68). Typical processing involves intercritical annealing after cold rolling, during which manganese partitions to austenite, increasing the austenite stability and leading to room temperature microstructures with high volume fractions (some up to approximately 60 vol%) of metastable austenite distributed in a high-strength fine-grained (on the order of 1 μm) ferritic matrix. The presence of retained austenite with controlled stability (i.e., enhanced resistance to deformation-induced transformation of austenite to martensite with strain) leads to steels that exhibit high strengths, high elongations, and excellent formability (53). Due to the use

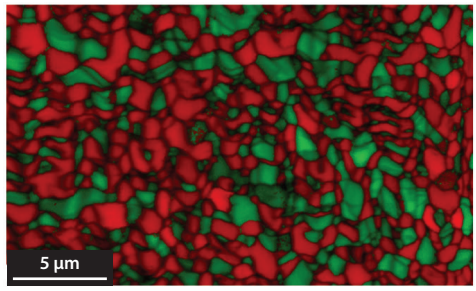

Figure 9

Electron back-scattered diffraction image quality map for 7 wt% Mn steel annealed at 620°C for 24 h to produce 40 vol% austenite (ferrite in *red*; austenite in *green*). Adapted with permission from Reference 70.

of manganese partitioning to stabilize austenite, the medium-manganese alloys typically have a lower carbon level relative to TBF and Q&P steels. For specific alloys, a thermodynamic-based model (69) can predict the amount of austenite that can be retained to room temperature and can thus guide the selection of processing temperatures.

Figure 9 shows the microstructure of a typical medium-manganese (nominally 7 wt% Mn) steel and illustrates the significant degree of microstructural refinement that is realized after intercritical annealing of a cold-rolled sheet (70). **Figure 10** illustrates the effects of annealing temperature on the transformation of austenite to martensite with strain and on the corresponding engineering stress-strain behavior (68). The austenite volume fraction varies from a high of 43.5 vol% for the sample annealed at 650°C to 1.4 vol% for the sample annealed at 675°C. The annealing temperature affects austenite composition, volume fraction, stability, and thus stress-strain behavior. Specifically, the sample annealed at 600°C exhibits 33 vol% austenite and stability

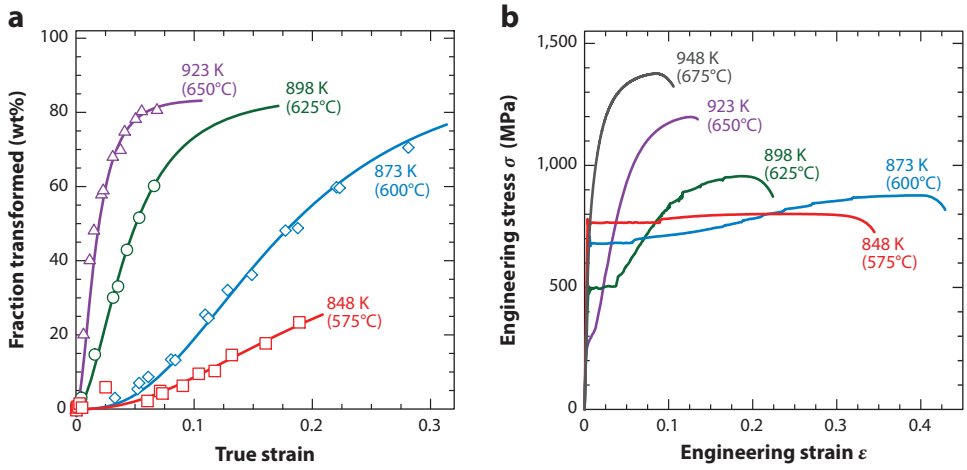

Figure 10

(*a*) Evolution of the fraction of austenite transformed to martensite with tensile deformation for different annealing temperatures ranging from 575°C to 650°C for 168 h, followed by water quenching. (*b*) Corresponding tensile stress-strain curves for 0.1 wt% C–7.1 wt% Mn–0.1 wt% Si samples. In both panels *a* and *b*, the samples contained the following initial retained austenite volume amounts: 1.4% at 675°C, 43.5% at 650°C, 40% at 625°C, 33% at 600°C, and 26% at 575°C. Adapted with permission from Reference 68.

with strain, as shown in **Figure 10*a***, leading to the excellent combination of strength and ductility shown in **Figure 10*b***. The breadth of properties illustrated by this example indicates that medium-manganese steels offer the opportunity to produce a wide variety of grades, all contained within the higher-ductility region of the third-generation AHSS band shown in **Figure 5**.

The examples considered here illustrate significant advances in the development of third-generation AHSS products. Other technologies to produce steels and steel products to enable lightweight designs include low-density steels, which contain aluminum contents up to approximately 10 wt% and base microstructures, depending on alloy additions, that are ferritic, austenitic, or multiphase (71). Density reductions up to approximately 12% have been realized. An alternate processing technology referred to as hot press forming utilizes boron-modified steels initially heated to a temperature to form austenite, followed by forming and quenching in a die to produce high-strength components (e.g., pillars and intrusion beams) critical to maintaining the integrity of the passenger compartment during a crash (72).

Advanced Bar and Forging Steels

Bar and forging steels are critical to automotive suspension systems, bearings, gears, shafts, etc. In powertrain components, e.g., transmissions, lightweighting is achieved by incorporating advanced steels with increased strength to facilitate higher-torque capacities in rotating shafts and enhanced resistance to bending and rolling contact fatigue in gears and bearings, leading to designs capable of higher power densities and thus smaller components for specific applications. While many advances have been made in microalloyed forging steels (73) and in carburized steels (74), steel processing developments that have led to cleaner steels and have thus facilitated the production of fatigue-sensitive components that operate at higher stress levels with longer lives are illustrated here (75–77).

During steel making, inclusions (brittle oxides, deformable sulfides, etc.) that form in liquid steel or on solidification may have detrimental effects on mechanical properties (e.g., toughness, fatigue resistance) and may thus limit the maximum allowable stresses that can be imposed on components. To maximize potential operating stresses, process modifications are utilized to minimize inclusion volume fractions and size. Fatigue cracks nucleate in steels (*a*) due to plastic deformation–induced damage to the microstructure; (*b*) at inclusions for a variety of reasons, including debonding (e.g., due to low interfacial strengths or due to high local stresses resulting from blocked slip bands); or (*c*) by inclusion fracture for brittle inclusions. On the basis of a fracture mechanics approach, Findley et al. (77) predicted the allowable fatigue stress as a function of inclusion size (represented here and in Reference 77 as the square root of inclusion area) (**Figure 11*a***). Also superimposed onto **Figure 11*a*** are typical yield stress levels for automotive components to illustrate that higher-strength components are more susceptible to fatigue. Application of inclusion control for high-performance bearings, critical to automotive lightweighting, has led to improved steelmaking practices that have resulted in cleaner steels, as illustrated in **Figure 11*b***, which correlates the fatigue life of bearings with inclusion content (expressed in the figure as the total length of inclusion stringers). Since 1980, improved steelmaking practices have led to a two-order-of-magnitude increase in fatigue life and steels produced on high-capacity mills, with properties equivalent to those of expensive vacuum arc remelted steels.

Thin-Wall Austempered Ductile Iron Castings

Ductile iron castings have long been an important material for automotive manufacture and remain a material of choice for many applications, in part due to the excellent castability exhibited by

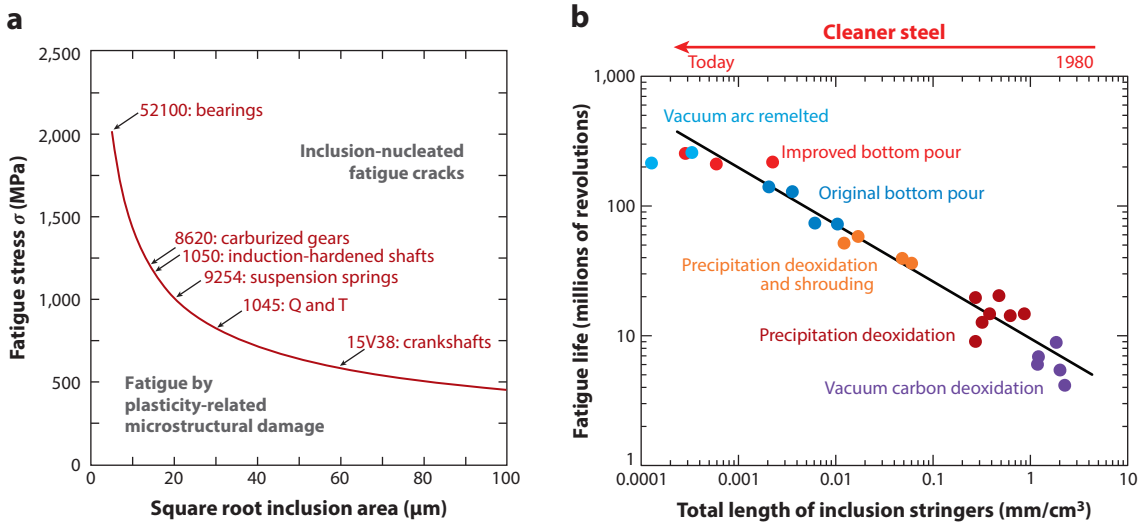

Figure 11

Effects of inclusion contents on (*a*) allowable fatigue stress and (*b*) bearing fatigue life. In panel *a*, the arrows indicate typical yield stress values for selected automotive components, and the corresponding conventional alloy designation is also shown. Stress levels above the line indicate fatigue nucleation by inclusions, while for stresses below the line, fatigue is controlled by the inherent resistance of the microstructure. In panel *b*, the different types of liquid steel processing are correlated with specific regions of the line. Panel *a* adapted with permission from Reference 77. Panel *b* adapted with permission from Reference 75.

iron casting, mechanical properties such as high strength-to-density ratios, and attractive cost (19). Recent advances in the production of thin-wall ADI castings have shown that ductile cast irons will be important materials to enable lightweight vehicle designs at a lower cost than for aluminum castings (78). ADI castings can also operate at higher temperatures with superior mechanical properties. In comparison to conventional cast iron products, alloys for thin-wall castings, which experience higher cooling rates associated with the smaller section sizes, typically have higher Si contents and utilize modified inoculation techniques to ensure the development of a high and uniform distribution of fine graphite nodules (79–81). As an example, **Figure 12** compares light

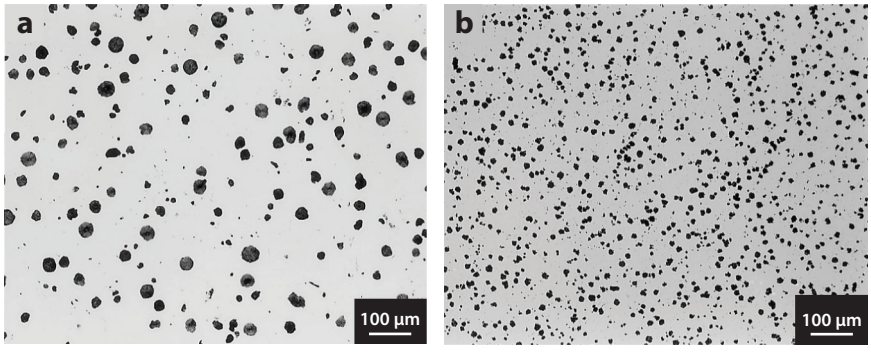

Figure 12

Light optical micrographs of unetched specimens that show the influence of section thickness on nodule count. (*a*) A 20-mm plate (150 nodules/mm^2). (*b*) A 2-mm plate (2,000 nodules/mm^2). Adapted with permission from Reference 80.

optical micrographs that show nodule densities in a cast iron treated with 2 wt% of FeSi9%MgCe and inoculated with 0.5 wt% of Fe75%Si and casting to produce either 20-mm plates (**Figure 12*a***) or 2-mm plates (**Figure 12*b***) (80). The 2-mm-thick sample exhibited a significantly higher cooling rate, leading to a higher degree of undercooling that enhanced nucleation. The result was a higher density of fine nodules relative to the 20-mm-thick sample. The effects of nodule count on mechanical properties are mixed. Stefanescu et al. (82) showed that tensile properties were independent of nodule count, while Górny & Tyrała (83) showed that strength increased with an increase in cooling rate, interpreted to reflect an increase in nodule count resulting from an increase in cooling rate. Further research is required to quantify the effects of nodule count and matrix microstructure on the critical properties (e.g., strength, toughness, fatigue resistance) required for lightweight automotive designs.

The examples included here illustrate that advances in steel alloy and process development are leading to new steels that can operate safely at higher stress levels and that therefore enable lightweight designs in multiple automotive applications. A couple of the major challenges for future materials research are below:

- Complete realization of enhanced properties illustrated by laboratory experiments using small-scale trial heats may require facility modifications or enhancements to apply the necessary processing histories.
- ICME tools need to be developed and/or refined to provide input to guide future alloy and process-history selections so as to further advance the recent developments illustrated here or to identify new material opportunities.

ALUMINUM AND MAGNESIUM

Aluminum and magnesium have a long history of automotive applications, as shown in **Figure 13** (84); however, extensive use of these materials began only in the mid-1970s. Both materials have seen steady growth since then, as more applications have been identified, largely due to increasing demands on vehicle fuel economy. The latest significant example is perhaps the use of aluminum body (approximately 318 kg lighter than the previous version) in high-volume production of 2015 Ford F-150 pickup trucks (85). The cost of the lighter-weight body is estimated to be consistent

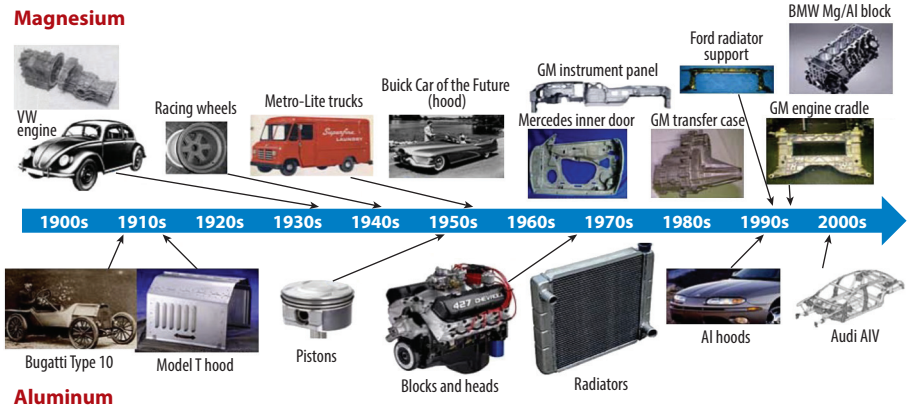

Figure 13

Timeline of key aluminum and magnesium automobile applications. Abbreviation: AIV, aluminum-intensive vehicle. Adapted with permission from Reference 84.

with the cost shown in **Table 2**. The average North American vehicle is estimated to contain approximately 187 kg of aluminum (86) and 10 kg of magnesium. The use of aluminum and magnesium will increase in the future, in part because of the increased demand for fuel economy and lightweighting and, more importantly, because of the development of innovative manufacturing processes and material improvements that should increase the capability of these materials and decrease the cost of using them. This section describes a number of manufacturing technologies that will enable increased use of aluminum and magnesium and discusses improvements in material properties or cost that may also increase the use of these materials.

Sheet Forming

Aluminum has lower formability relative to the low-carbon steel materials used to stamp most automotive body structures and closures. Thus, aluminum has been extensively used only for hoods, which are relatively simple to stamp. For more complex stampings, like door, liftgate, or decklid inner panels, one must either use a multipiece approach or use a nontraditional, hot forming technology like quick plastic forming (87). Sheet magnesium has not been used for even simple panels, due to its extremely low formability, which is even lower than that of aluminum. However, prototype components have been successfully made using hot blow forming technologies like quick plastic forming, and low-volume application of magnesium has been realized (88). Multipiece assemblies or hot blow forming technologies are expensive, and there is a desire to develop high-volume technologies that can produce complex aluminum and magnesium panels at volumes of more than 30,000 per year. The forming technologies described here should enable forming of complex aluminum and magnesium panels at medium to high volumes.

Warm forming involves stamping sheet materials at 200°C to 350°C, resulting in the significantly enhanced formability of 5xxx series aluminum and magnesium alloys (89, 90). The process uses heated, matched die sets and conventional stamping rates (5–10 jobs/min). This enables high-volume production using existing press infrastructure, which is attractive in the current market, in which a lot of excess capacity exists. Warm forming has been studied for more than 40 years in prototype shops and laboratories (91) but has not been commercially utilized at any significant level. This lack of use is due to difficulties in controlling the heat distribution and dimensions in the die, as well as the lack of a suitable lubricant and rapid blank heating technique. There has also been some resistance to using thermal stamping technologies in conventional press shops. Recent work has demonstrated successful stamping of an aluminum and magnesium inner door panel and identified new lubricants, which could work in the warm forming process (84). In addition, the continued acceptance of press quenching for steel suggests that there may be more opportunities for thermal stamping technologies. The continued development and ultimate implementation of a warm stamping technology would enable greater opportunities for the use of aluminum and magnesium in complex stampings, especially in inner door panels.

Tube Hydroforming

Tube hydroforming uses pressurized fluids such as water to make fairly complex perimeter shapes from simple-geometry tubes. Hydroformed parts have replaced assembled and welded stamped components and generally achieve a mass savings of 15–20% and accompanying cost savings due to part consolidation, elimination of welding flanges, more efficient section design, reduced wall thickness, lower-cost tooling, and fewer processing steps due to the combination of

Figure 14

Hydroformed aluminum rail for the Corvette Z06 shown immediately after forming. Reproduced with permission from Reference 92.

forming and piercing. Although hydroformed steel subsystems are used pervasively in automotive applications, the conversion to aluminum, and subsequently to magnesium, has been slow. The largest hydroformed part in the world is the 4.8-m-long aluminum frame rail for the Corvette (92). These tubes, shown immediately after forming in **Figure 14**, saved 20% of the mass from the steel rails that they replaced. The ongoing research challenge is to further reduce the weight and cost of hydroforming aluminum parts by utilizing ICME optimization.

Castings

Aluminum can be cast by many processes, including precision sand casting coupled with low-velocity fill, low-pressure die casting, permanent mold casting, and high-pressure die casting (HPDC). For magnesium, HPDC is the dominant technology. Future growth of both aluminum and magnesium will depend on additional casting process developments. We now discuss two technologies that may have a significant impact on aluminum and magnesium use in the future.

High-vacuum die casting processes have emerged that are capable of producing components that exhibit minimal porosity and are heat treatable and weldable, thus overcoming the two largest shortcomings of traditional HPDC. New aluminum alloys, such as AURAL-2, Silafont-36, and Magsimal-59, have been specifically developed for high-vacuum die casting processes (93, 94). A vacuum-assisted die casting process has also been developed for producing magnesium alloy components with reduced porosity (95). The subsequent development of super-vacuum die casting (SVDC) parts (96) demonstrates a 50% increase in ductility relative to conventional HPDC components.

SVDC processes are expected to gain increased popularity as more castings become incorporated into structural subsystems along with the possibility of casting thinner sections with higher integrity relative to HPDC for additional mass reduction. An example application is the cast aluminum shock tower for the Cadillac ATS sedan, which weighs 2.8 kg and represents a weight savings of approximately 50% relative to a comparable design of sheet-steel construction (29). Developments are also expected in squeeze casting, as enhanced properties will become expected from castings that have thick sections, such as wheels and control arms. The properties of these high-integrity castings are approaching those of forgings, but at substantial cost savings.

One important requirement for these structural castings is high ductility (>10% elongation), which is needed for joining processes (typically self-pierce riveting). Iron is a common impurity element and can form a brittle iron-rich intermetallic phase known as β-Al_5FeSi in cast aluminum alloys. However, a certain level of iron is desired in cast aluminum alloys for HPDC since it reduces the tendency of die soldering and improves the hot tearing resistance (97, 98). It is a

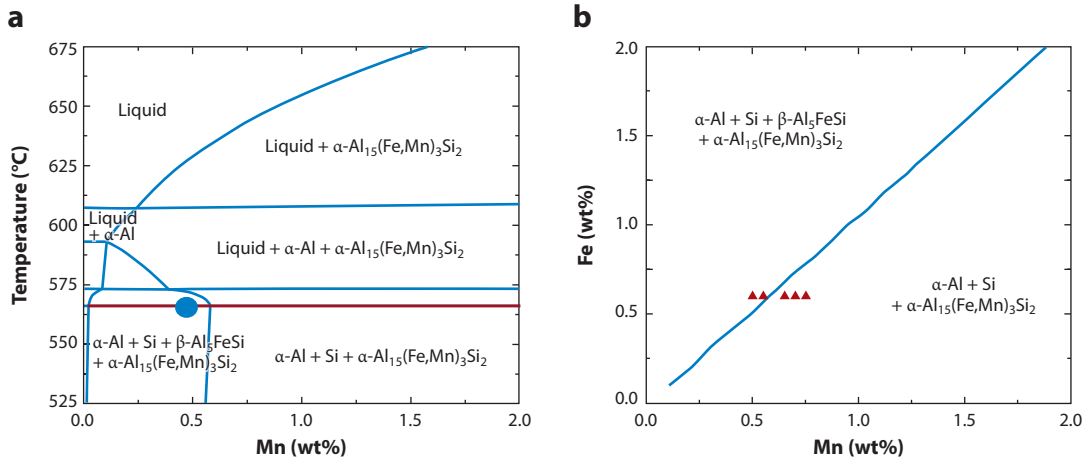

Figure 15

(*a*) Calculated isopleth for Al–8 wt% Si–0.35 wt% Mg–0.6 wt% Fe–*x*% Mn. (*b*) The effect of Fe and Mn content on the formation of the β-Al_5FeSi intermetallic phase in the Al-Si-Mg-Fe-Mn alloy system. Figure adapted from Reference 101.

common practice to add manganese to aluminum alloys to modify β-Al_5FeSi intermetallics. Numerous studies on the modification effect of manganese and cooling rate on iron-rich intermetallic phases have been reported for several alloy systems (98–100). A recent study (101), based on CALPHAD (CALculation of PHAse Diagrams) modeling of the Al-Si-Mg-Fe-Mn system, reveals the relationship between the iron concentration and the required level of manganese to eliminate the β-Al_5FeSi phase (**Figure 15**). The simulation results and experimental validation suggest that an iron-to-manganese ratio of less than 1 can effectively eliminate the β-Al_5FeSi phase in the as-cast microstructure. This finding forms an important basis for controlling the ductility of aluminum castings.

Research has been focused on thin-wall aluminum and magnesium casting development (**Figure 16**) through alloy optimization and advanced process simulation (104). The research has developed key process technologies (SVDC and shortened heat treatment) and ICME tools for

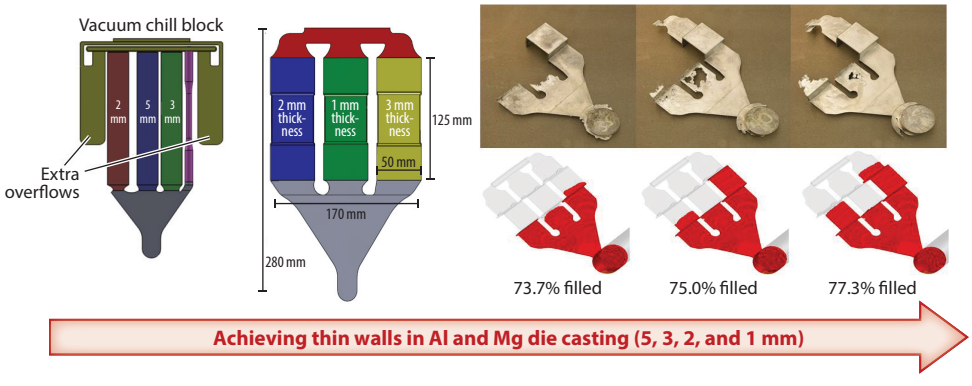

Figure 16

Achieving thin-wall aluminum and magnesium die casting through alloy optimization and process simulation. Adapted from Reference 102.

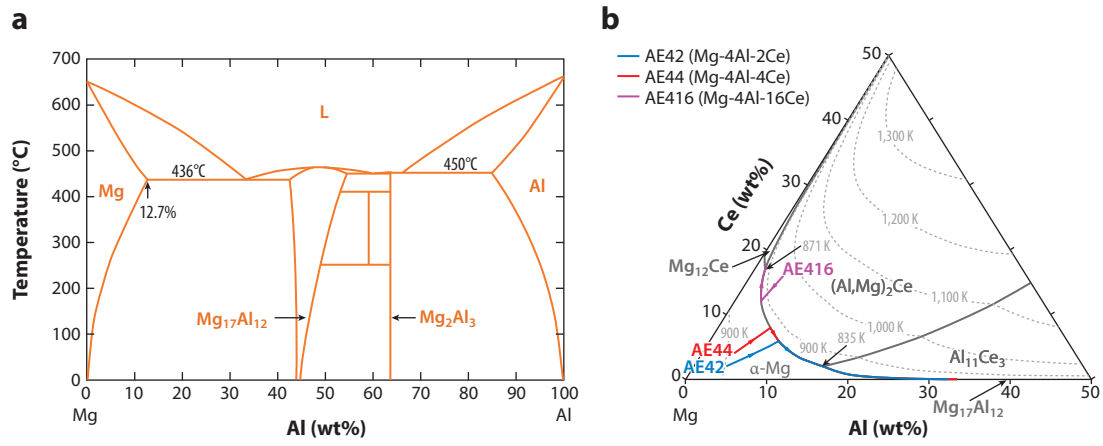

Figure 17

(*a*) Calculated Mg-Al phase diagram. L denotes liquid. (*b*) Calculated Mg-Al-Ce liquidus projection and solidification paths of experimental Mg-Al-Ce alloys. Panels *a* and *b* adapted from Reference 103.

300 series (Al-Si-Cu-Mg-based) die casting alloys to improve mechanical properties and to reduce the minimum wall thickness (by up to 40%) and weight (by up to 20%) of these die castings.

Alloy Development

Over the last few decades, many new aluminum and magnesium alloys (cast and wrought) have been developed for automotive applications. The following provides one example (103) of how the CALPHAD approach is used to design a high-temperature magnesium alloy for automotive engine cradle application.

Aluminum is the most widely used alloying addition to magnesium for strengthening and castability. **Figure 17*a*** shows a calculated Mg-Al phase diagram. The low eutectic temperature (436°C) of the $Mg_{17}Al_{12}$ phase limits the application of Mg-Al alloys to temperatures below 125°C, above which the discontinuous precipitation of the $Mg_{17}Al_{12}$ phase leads to substantial creep deformation. Therefore, possible approaches for improving creep resistance in Mg-Al-based alloys include (*a*) suppressing the formation of the $Mg_{17}Al_{12}$ phase, (*b*) pinning grain boundary sliding, and (*c*) slowing solute diffusion in the magnesium matrix.

Figure 17*b* shows the calculated liquidus projection of the Mg-Al-Ce system in the Mg-rich corner. The additions of 2–4% Ce to Mg-Al alloys result in the formation of $Al_{11}Ce_3$ and reduce the formation of the $Mg_{17}Al_{12}$ phase in the Mg-Al binary system. The calculations also show that approximately 15% Ce (which is too expensive) is required to completely suppress the formation of the $Mg_{17}Al_{12}$ phase in the Mg-4Al alloy. Thus, the AE44 (Mg-4Al-4Re) alloy was selected for the Corvette engine cradle application, for which the operating temperature would approach 150°C (105).

Some of the major challenges for future materials research in aluminum and magnesium alloys are:

- alloy development for higher specific properties (including metal matrix composites with nanosized reinforcements) and low costs (including using secondary alloys);
- innovative casting processes, including high-integrity processes and semisolid processes;
- improved forming processes, such as warm and hot forming and sheet hydroforming; and
- additive manufacturing and dissimilar material joining processes.

POLYMER COMPOSITES

Fiber-reinforced polymer composites are key enablers of energy efficiency gains and emissions reductions. High strength-to-weight ratios, exceptional durability, and directional properties are some key benefits of polymer composite materials as valued choices for high-performance automotive applications. The low-cost, energy-efficient production of advanced fiber-reinforced polymer composites is expected to revitalize US manufacturing and innovation and to yield substantial economic and environmental benefits. Advances in material intermediates and manufacturing technologies are needed for increased use of polymer composites in the automotive industry.

Present Applications of Polymer Composites

There are several opportunities for plastics and polymer composites for lightweighting and energy efficiency in vehicles (104). Representative applications are illustrated in **Figure 18** and include the following:

- Automotive body exterior: Bumpers, roof surrounds, and body horizontal and vertical panels made from composites provide lighter vehicles with better gas mileage and allow designers and engineers the freedom to create innovative concepts. Polymer composites for automotive body exterior panels and parts allow for modular assembly practices; lower production costs; improved energy management; better dent resistance; and the use of advanced styling techniques for sleeker, more aerodynamic exteriors.
- Automotive interior: Polymers and polymer composites provide comfort, reduced noise level, aesthetic appeal, ergonomic layout, and durability.
- Automotive safety: Composite structures in the front end of a vehicle absorb energy while lowering vehicle weight. Plastics are also used in door modules to maintain or improve side

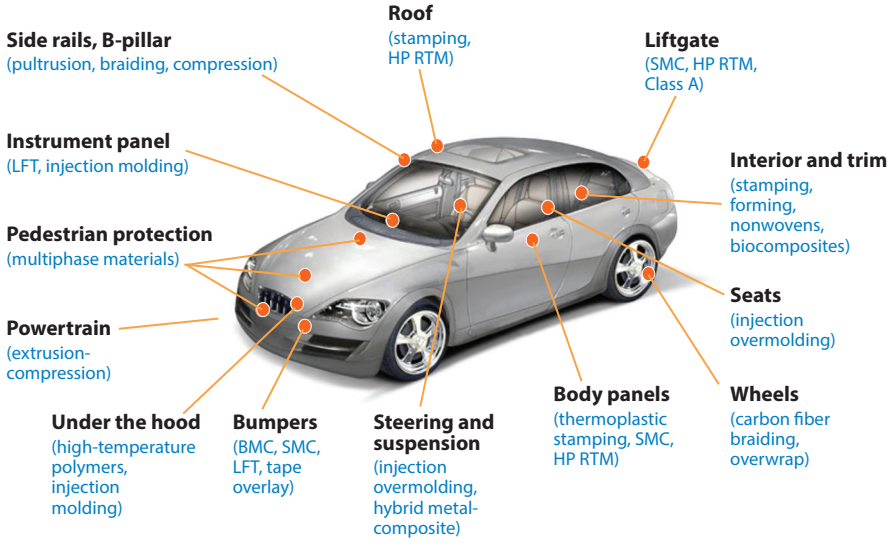

Figure 18

Comprehensive opportunities for polymers and polymer composites with associated manufacturing processes for lightweighting in vehicles. Abbreviations: BMC, bulk molding compound; HP RTM, high-pressure resin transfer molding; LFT, long-fiber thermoplastic; SMC, sheet molding compound. Adapted from Reference 105.

impact safety, as layers in automotive safety glass to prevent passenger injuries, and as polymer foams that add strength to automotive body cavities and increase occupant safety in vehicles.

- Automotive electrical systems: Polymers and polymer composites are used in interconnections and housings for sockets, switches, connectors, circuit boards, wiring and cable, and other electrical and electronic devices.
- Automotive chassis: Polymers can be used in chassis support and suspension structures due to their high performance in energy absorption and in reducing noise and vibration.
- Automotive powertrains: The powertrain includes the system of bearings, shafts, and gears that transmit the engine's power to the axle. Powertrain is one of the most difficult systems for lightweighting, but overmolding long-fiber thermoplastics (LFTs) with cast metals can be used to deliver increased torque at lower weight.
- Automotive fuel systems: Composites offer more design freedom over conventional metals. High-performing automotive fuel tanks and related delivery systems incorporate leak-proof, corrosion-resistant, and reliable compressed natural gas tanks. The overbraiding of filament wound tanks enhances the burst resistance of CNG tanks and absorbs energy.
- Automotive engine components: Relevant engine components include air-intake manifolds, cooling system components, and valve covers. Plastics are in use to make engine systems easier to design, easier to assemble, and lighter in weight.

Today approximately 10–15% of a vehicle is manufactured from polymers and composites. These materials can improve passenger safety and provide design flexibility. The parts include instrument panels, seat components, interiors, underbody structures, trunks, underhood components, and door inners. **Figure 19** illustrates the increasing use of polymers and polymer composites in vehicles today. Polypropylene is the dominant material used due to its low cost (**Figure 20**). There is increased interest in thermoplastic resins and use of recycled fibers. In terms of reinforcements, E-glass fiber is widely used due to low cost and high performance. Lighter weight, lower embodied energy, increased recyclability, and high performance are the key drivers for carbon and natural fibers.

Carbon Fibers

Advances in carbon fiber technologies via alternative precursors, efficient processes, and interface engineering enable cost reduction at improved performance. Alternative precursors such as textile-grade polyacrylonitrile and processing approaches are being adopted to engineer carbon fiber materials that yield superior final part properties at reduced production energy levels. The

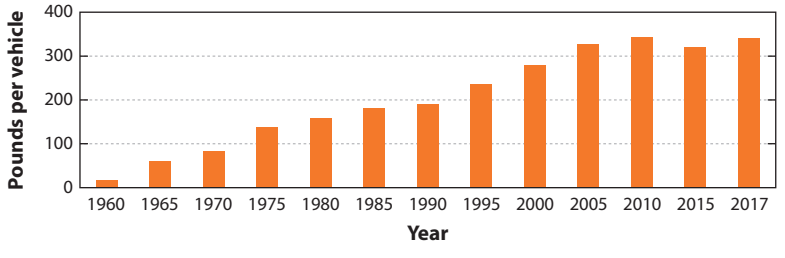

Figure 19

Historical average material usage of various plastics and composites in US and Canadian light vehicles. Adapted from Reference 104.

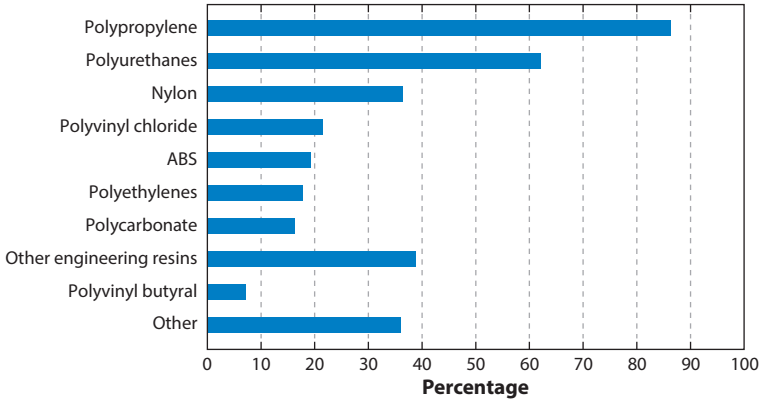

Figure 20

Average plastics and polymer composites use in US/Canadian light vehicles. ABS denotes acrylonitrile butadiene styrene. Adapted from Reference 104.

Department of Energy (DOE) set a target for low-cost (textile-grade) carbon fiber [or textile carbon fiber (TCF)] at 1,700 MPa tensile strength and 25 Msi tensile modulus. Recent advances have enabled TCF at properties and cost metrics exceeding these set metrics for automotive adoption (106). Recent developments in TCF have enabled fiber properties at 2,800 MPa tensile strength and 260 GPa tensile modulus with a potential cost of $10/kg.

The TCF has a 457,000–600,000 filament count (shown in **Figure 21**), which is analogous to a sheet, in contrast to a commercial 12,000–50,000-filament fiber (for example, ZOLTEK PX 35). **Table 3** shows representative properties of the TCF-based epoxy composites. The strength and modulus of the TCF exceed those required for automotive applications.

Polymer Composite Processing

Innovative reinforcements, resins, additives, and intermediates are enabling fast cycle times, reduced scrap, integrated features, and reduction in embodied energy. Integrated fabrics, preforms, and prepregs are used in fast-cycle-time production of composites such as door inners, floors, seat backrests, roofs, trunks, and underhood auto components. Advanced manufacturing techniques, including injection overmolding (IOM), stampable preforms, wet compression, locally stitched preforms, high-pressure resin transfer molding (HP RTM), and extrusion-compression, are

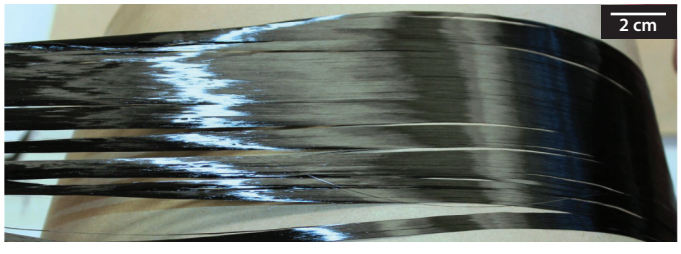

Figure 21

Wide-tow textile-grade carbon fiber produced at the Carbon Fiber Technology Facility at Oak Ridge National Laboratory. Reproduced from Reference 106.

Table 3 Representative properties of textile carbon fiber (TCF) epoxy composites[a]

Property (cross-ply)	TCF (66% volume fraction, V_f) epoxy
Tensile strength	548 MPa (79.48 ksi)
Tensile modulus	84 GPa (12.18 Msi)
Flexural strength	655 MPa (95 ksi)
Flexural modulus	73 GPa (10.6 Msi)
Compression strength	456 MPa (66.1 ksi)
Compression modulus	72 GPa (10.4 Msi)
Interlaminar shear strength	45 MPa (6.5 ksi)

[a]TCF represents a family of fibers depending upon the precursors. These properties represent those generated by IACMI in the 2016–2017 period. There are continuing efforts to enhance precursors, with the goal of increasing the TCF properties.

examples that reduce composite manufacturing costs and energy consumption and improve component performance and recyclability.

In HP RTM, continuous fabrics and discontinuous nonwovens are preformed to optimized blanks and are placed in a production closed cavity tool (**Figure 22**). Low-viscosity resin is injected at high pressures ranging from 8 to 12 GPa; the resin rapidly permeates through the preform (typically in less than 1 min) to cause full wet out and rapid curing times ranging from 30 to 180 s (107, 108). The glass transition temperatures of these systems are in the range of 120°C to 130°C.

In wet compression, the preform is placed in the tool cavity, and low-viscosity resin is robotically delivered to the preform (109) (**Figure 23**). The press is then closed on the cavity, and the resin infiltrates the preform, much like in RTM. Darcy's law applies for the flow of the resin in the tool cavity. Permeability of the fabric, weave architecture, ply thickness, and part geometry need to be optimized to influence the flow and minimize the fill rate.

IOM is being used more extensively in automotive components such as door inners, bumper beams, instrument panels, and crash members. In IOM, a thin layer of continuous fabric preforms or tapes provides the structural load-bearing elements, and complex features such as ribs, bosses, and steps are back molded with a high-performance polymer and/or LFT such as glass or carbon polyamide 6 (PA6-C) (110–112). The advantage of this approach is the ability to achieve highly

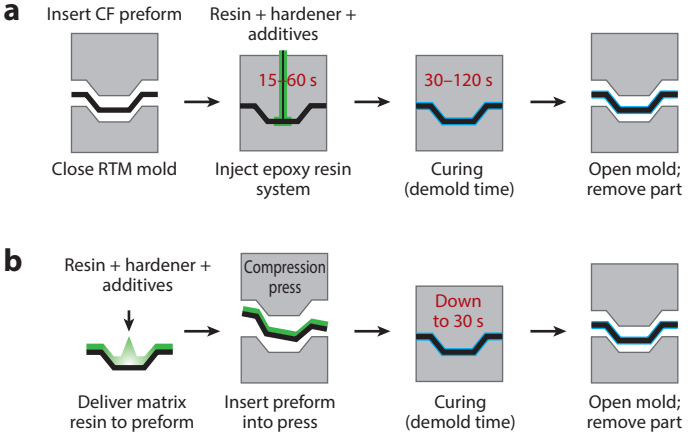

Figure 22

(*a*) High-pressure resin transfer molding (RTM). CF denotes carbon fiber. (*b*) Wet compression processing.

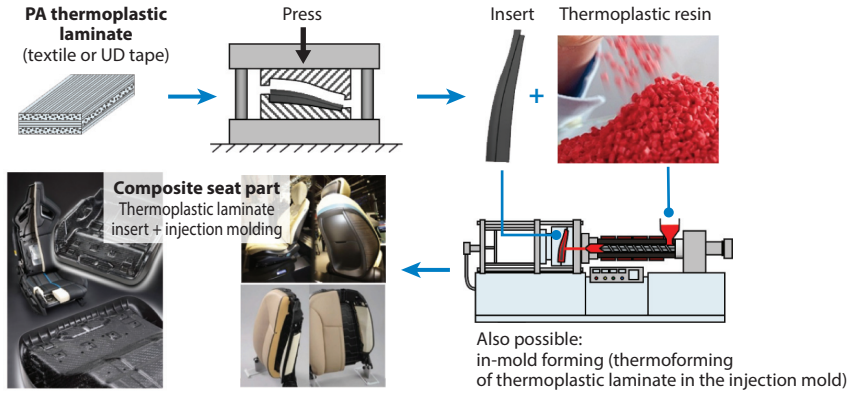

Figure 23

Overmolding steps of automotive components. Abbreviations: PA, polyamide; UD, unidirectional. Figure adapted courtesy of BASF.

complex, near-net shapes in cycle times of less than 90 s. **Figure 23** illustrates the cycle of a part produced with this process (110). **Figure 24** illustrates a PA6-C LFT compared to an overmolded PA6-C LFT. A 275% enhancement of load bearing and strain capacity is observed by utilizing a single layer over an LFT substrate (111).

LayStitch is a related development in composite preforming for overmolding. In LayStitch, the fiber mats are locally reinforced through automated stitching of high-strength fibers. The resulting composite can bear strength for postassemblies such as fasteners or bear high stress at local points (113).

Prepreg stamping uses preimpregnated thermosets and thermoplastics much like those used by the aerospace industry. To be economical in automotive applications, prepregs made from glass, carbon, and basalt reinforcements in epoxy, vinyl ester, or thermoplastic resins can be preformed readily and compression molded at rates approaching those of stamping metal sheets. Near-net-shape parts are realized through this process. Prepreg technologies are fairly broad, including wetting of reinforcement of thermosets, hot melt impregnation, and solvent-based thermoplastic

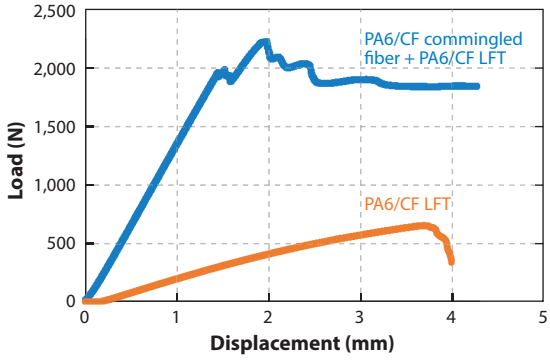

Figure 24

Comparison of carbon PA6 versus overmolded carbon PA6. The latter shows a 275% increase in load bearing. Abbreviations: CF, carbon fiber; LFT, long-fiber thermoplastic; PA6, polyamide 6. Adapted from Reference 111.

prepregs. The fiber volume is controlled accurately, ranging from 50% to 62% by volume, and can be further tailored as desired (114).

LFTs can be injection and/or extrusion-compression molded. The long-fiber pellets made from a range of fiber-resin combinations, such as polypropylene (PP), polyamide (PA), polyphenylene sulfide (PPS), or thermoplastic polyurethane–glass fiber (TPU-GF), are used in this process. The pellets are produced through hot melt impregnation or pultrusion of rods that are pelletized to a length of 12 to 25 mm (115, 116). The conveying screw in injection or extrusion has a low-shear design to minimize fiber attrition. In fiber injection molding, pellets that are 12 mm or shorter melt and disperse in the extruder and are forced through the nozzle to flow in the cavity. The fiber length is highly directional in this process (117).

In extrusion-compression molding (ECM), the LFT pellets are fed through a low-shear screw to produce a high-viscosity fiber-resin charge. The charge is transferred to a fast-acting press that houses the mold (the tool). The part is produced in 1–3 min by compression molding of the charge. **Figure 25** illustrates the fiber orientation and properties of an ECM and IM part.

Sheet molding compounds (SMCs) have widescale use in automotive applications. In SMCs, glass, basalt, carbon, and natural fiber reinforcements are chopped on a rotary cutting system. Polyester and vinyl ester with additives such as talc are fed through doctor boxes on either side of the chopped fibers to form resin film and to sandwich the fibers into a tacky nonwoven form. The material has approximately 6 weeks of shelf life and can be cut to preform. SMCs are compression molded at 7–8 GPa to flow and form the part at temperatures of 150–175°C. Components such as tailgates, seat backrests, and fenders are produced with SMCs. **Figure 26** illustrates a seat backrest component molded with a structural SMC material in a cycle time of 45 s (118, 119).

Recycling of Polymer Composites

Recycling of composites is of growing interest due to the possibility of low-cost carbon fiber integration into automotive designs. Since recycled chopped carbon fiber costs 70% less to produce and up to 98% less energy to manufacture than virgin carbon fiber, recycling technologies can create new markets for the estimated 29 million pounds of composite scrap sent annually to landfills. Advances in recycling technologies, including pyrolysis, solvolysis, mechanical shredding, and thermolysis incineration, are enabling recycle, reuse, and remanufacture of products (120–125).

Drop-in recycled intermediates are made in wet laid or air laid mats more than 1 m wide (**Figure 27**). A recycled carbon fiber mat can be configured for various proportions. For example, a PA6-C mat may be in proportions of 30 wt% carbon and 70 wt% PA6 fibers. The mats

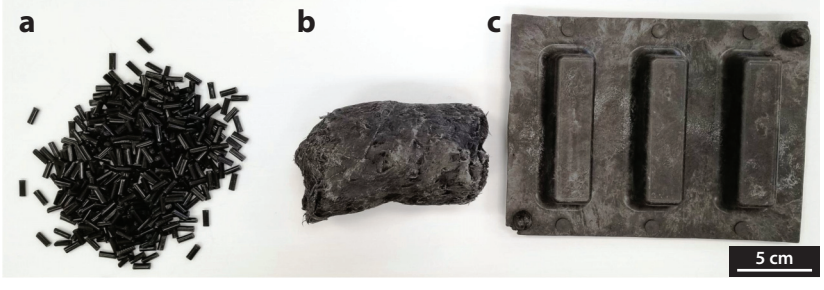

Figure 25

Material stages in the long-fiber thermoplastic–extrusion-compression molding process: (*a*) polypropylene glass fiber pellets, (*b*) plasticated charge, and (*c*) compression-molded plate. Reproduced from Reference 115.

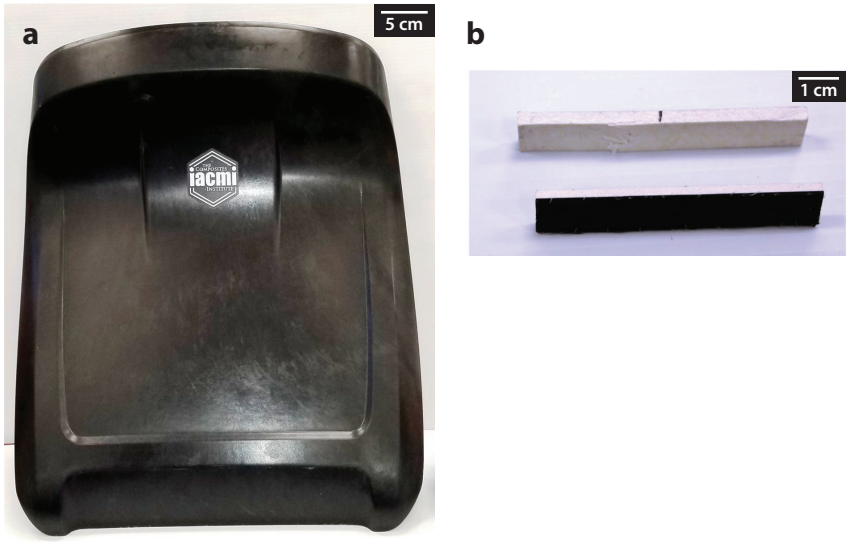

Figure 26

(*a*) Molded sheet molding compound (SMC) seat backrest at a cycle time of 45 s. (*b*) SMC molded plaque and overmolded SMC plaque.

typically range from 80 to 500 g/m^2 and can be processed by producing preconsolidated panels and by compression molding these panels to shape. In some cases, the mats are passed through an infrared oven and stamped to shape in the mold. **Table 4** summarizes representative properties from recycled carbon fiber composites.

Recycled carbon fibers can also be used in twin screw produced, compounded pellets in various concentrations. The carbon fiber polymer pellets, such as PA6-C, PP-C, and PP–acrylonitrile butadiene styrene, are then used as feedstock for injection molding, extrusion-compression, or

Figure 27

Example of a recycled carbon fiber polyamide 6 (PA6) mat that can be stamped/compression molded to near net shape.

Table 4 Representative properties of recycled carbon fiber mats in polyamide 6 (PA6) and epoxy resin systems

Property (cross-ply[a])	Carbon-PA6 (28% volume fraction, V_f), 1" fiber length	Carbon-epoxy (26% volume fraction, V_f), ½" fiber length
Tensile strength (MPa)	460 MPa (66.7 ksi)	225 MPa (32.6 ksi)
Tensile modulus (MPa)	24.2 MPa (3.5 Msi)	20 MPa (2.9 Msi)
Flexural strength (MPa)	465 MPa (67.4 ksi)	310 MPa (45 ksi)
Flexural modulus (GPa)	23 GPa (3.3 Msi)	18 GPa (2.6 Msi)
Interlaminar shear strength (MPa)	49 MPa (7.1 ksi)	42 MPa (6 ksi)

[a]Cross-ply here refers to the lay up of mat layers alternating in the machine direction and the cross direction.

extrusion deposition additive manufacturing. Studies have shown that the number of times that the shredding-processing can occur ranges from 5 to 7 cycles, depending upon the polymer.

Additive technologies in composite manufacturing are providing innovative pathways such as 3D printing of components for full vehicle bodies. The Oak Ridge National Laboratory (ORNL) Manufacturing Demonstration Facility (MDF) has demonstrated BAAM (big-area additive manufacturing) for 3D printing by extrusion deposition of Strati (**Figure 28*a***), Shelby Cobra, Jeep Willys, and military vehicle hoods, to name a few. Additive manufacturing offers a high-rate, low-cost alternative to traditional toolmaking for compression and resin transfer molding to produce prototypes (**Figure 28*b***). Additive manufacturing of polymer and metal tools is reducing the lead times for prototype development. Automated tape placement enables hybrid processes with additive manufacturing through local tape placement in conjunction with extrusion deposition or fused deposition printing.

Advanced Resins

Both thermoset and thermoplastic resins are being customized for automotive use. Fast-curing epoxies, unsaturated polyesters, and vinyl ester thermosets with environmentally friendly chemistries, reduced volatile organic compounds, and reduced or no styrene content are enabled.

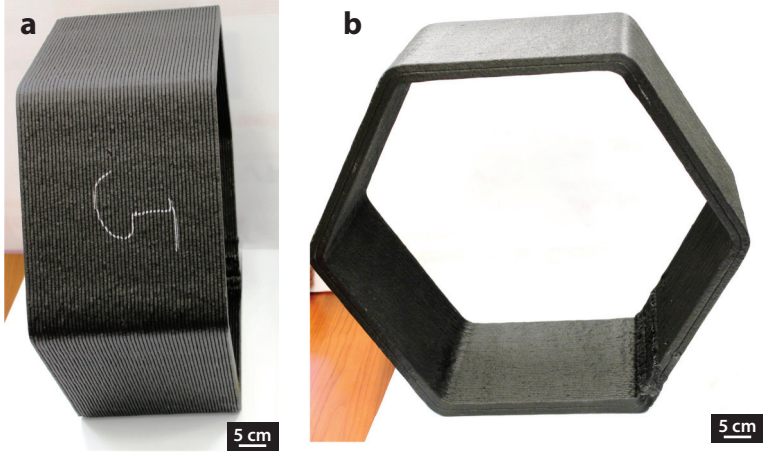

Figure 28

Hexagonal geometry section of a Strati car produced on the BAAM (big-area additive manufacturing) printer at the Manufacturing Demonstration Facility at Oak Ridge National Laboratory. (*a*) Side view. (*b*) Cross section.

These resins are being used in filament winding, pultrusion, HP RTM, prepregs, and wet compression processes. Thermoplastics provide the recycling benefit and higher energy absorption for crashworthiness. Thermoplastics in the automotive industry include olefins (PP, polyethylene), PA6, PA66, polycarbonate, polybutylene terephthalate, and TPU for structural and semistructural components and high-temperature PPS, polyethylenimine, and polyether ether ketone for underhood applications. Liquid molding thermoplastics with poly(methyl methacrylate) chemistries are also being used with carbon fibers. Increasing the use of thermoplastics requires research advances in the development of novel in situ polymerization methods to improve thermoplastic fatigue performance and the establishment of design-for-recyclability methods.

Advanced Modeling for Design

Design, prototyping, and validation are integral steps for turning conceptual designs into high-performance components and verifying that these components meet their intended product requirements. These product development steps rely on a robust understanding of material limits; processing capabilities; principles of mechanical design; and best manufacturing practices to optimize the safety, reliability, and performance of a system.

Advances are needed in design optimization approaches, including those for manufacturability and recyclability, validation of composite crash simulation models, and creation of techno-economic analyses of automotive composite parts to provide manufacturers with design, prototyping, and validation examples. Advances are also needed in modeling and simulation tools for automotive applications, including assessing variability in end-to-end simulated manufacturing processes, conducting accelerated tests and validating models with experimental data, incorporating composite joint designs into crashworthiness models, and sharing key material properties to inform simulation efforts. The integration of these efforts can enable reductions in product development times (**Figure 29*a***). The Composites Design & Manufacturing HUB and the Composites Virtual Factory HUB at IACMI Purdue University enable modeling and simulation for a range of manufacturing scenarios. Various manufacturing modules developed by the team include prepreg stamping, fiber flow in injection molding, draping, and additive manufacturing. **Figure 29*b*** illustrates representative work in modeling of layer-by-layer extrusion deposition by the ORNL MDF team to evaluate local thermal stresses developed in the components during processing.

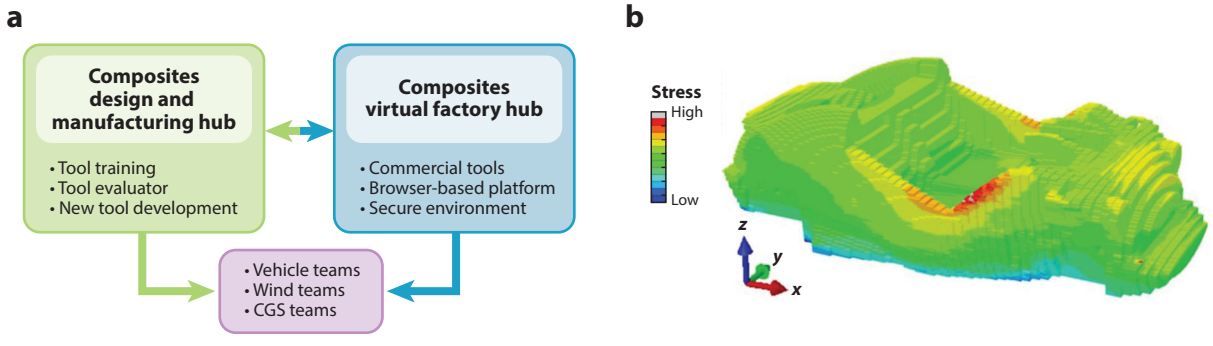

Figure 29

(*a*) Modeling and simulation hub at IACMI Purdue University with a comprehensive set of capabilities for prepreg stamping, injection molding, compression, and additive manufacturing. CGS denotes compressed gas storage. (*b*) Model of local thermal stresses developed in layer-by-layer extrusion deposition of acrylonitrile butadiene styrene material.

Several enabling technologies are emerging for polymer composites in the automotive industry. The technologies enable reductions in embodied energy (126–128), reductions in life cycle costs, recyclability, and reductions in manufacturing costs. Some of the major challenges for incorporating polymer composites into vehicles include developments in low-cost carbon fibers; design, modeling, and simulation; process innovations; hybrid materials; enhanced energy absorption; nondestructive evaluation; and recycling technologies.

MULTIMATERIAL JOINING

Multimaterial joining is increasingly important as automotive designs are evolving heavily into multimaterial designs. Instead of designing complex systems with single-material solutions, manufacturers rely on multimaterial design approaches to selectively integrate advanced materials into components without imposing a significant technology implementation risk (126, 129, 130). Increasing the technological maturity and acceptance of multimaterial joining techniques is essential to their widespread use across the manufacturing industry. Multimaterial joining is therefore a crucial enabling technology for the integration of steel, aluminum, magnesium, and high-performance composite components.

The area is guided by a couple factors. First, regarding material selection and design tools, the manufacturing industry requires robust design tools, reliable test methods, and best practices to ensure that novel multimaterial joining techniques are sufficiently cost effective and dependable to achieve design compliance and serviceability and to meet end-of-life requirements of key applications. Research is focused on (*a*) assessing multimaterial joining approaches for scale-up (e.g., welding, adhesive, mechanical joining), (*b*) developing accelerated aging tests for mixed-material joints to generate lifetime performance data, and (*c*) developing third-party data evaluation approaches and incentivizing original equipment manufacturer data sharing via access-controlled databases.

Second, regarding monitoring, inspection, and repair, new materials and innovative designs for enhancing product performance are creating a constant demand for novel nondestructive examination inspection methods, state-of-the-art instrumentation, and skilled inspectors capable of synthesizing and interpreting measurement data. Robust sensing and inspection methods are essential for assessing the integrity, repairability, and producibility of multimaterial joints in key lightweighting applications. These methods include (*a*) creating structural health monitoring reference/training materials for different job functions and (*b*) developing defect detection techniques (e.g., ultrasound) that can test frequencies of the entire structure.

SUMMARY

The automotive industry has transitioned from an era of maintaining vehicle weight to delivering significant weight reduction in newer models. Optimizing the vehicle structure for weight minimization requires using a variety of materials produced by different methods into the correct form and then joining those components. This review identifies key research challenges ranging from the need for new alloys and polymers to development of lower-cost processing technologies. The increasing availability of new ICME models will enable faster and more efficient research in these areas.

DISCLOSURE STATEMENT

The authors are not aware of any affiliations, memberships, funding, or financial holdings that might be perceived as affecting the objectivity of this review.

ACKNOWLEDGMENTS

The authors wish to recognize support from the Office of Naval Research under LIFT, from the Department of Energy under the IACMI, and from the industrial sponsors of the Advanced Steel Processing and Products Research Center at Colorado School of Mines. The authors would like to thank Ellen Kampf, University of Michigan, for her assistance in preparing the manuscript.

LITERATURE CITED

1. US Natl. Res. Counc. 2003. *Materials Research to Meet 21st Century Defense Needs*. Washington, DC: Natl. Acad. Press
2. Roeth M. 2015. *Confidence report: lightweighting*. Rep., North American Council for Freight Efficiency. **https://nacfe.org/technology/lightweighting-2/**. Accessed Nov. 20, 2017
3. Taub AI, Krajewski PE, Luo AA, Owens JN. 2007. The evolution of technology for materials processing over the last 50 years: the automotive example. *JOM* 59(2):48–57
4. Schutte C, Joost WJ. 2014. *Lightweight materials for cars and trucks*. **https://www.energy.gov/eere/vehicles/lightweight-materials-cars-and-trucks**
5. Joost W. 2015. *Energy, materials and vehicle weight reduction*. Rep., US Dep. Energy. **http://www.nist.gov/mml/acmd/structural_materials/upload/Joost-W-DOE-VTP-NIST-ASP-AHSS-Workshop-R03.pdf**
6. Picker L. 2017. *Vehicle weight and automotive fatalities*. Digest, NBER. **http://www.nber.org/digest/nov11/w17170.html**. Accessed Dec. 3, 2017
7. Plumer B. 2014. Cars in the US are more fuel-efficient than ever. Here are 5 reasons why. *Vox*, Sept. 4. **https://www.vox.com/2014/9/4/6107203/cars-in-the-us-are-more-fuel-efficient-than-ever-here-are-5-reasons**. Accessed Dec. 3, 2017
8. US Envir. Prot. Agency (EPA). 2015. *Light-duty automotive technology, carbon dioxide emissions, and fuel economy trends: 1975 through 2015*. Rep., US EPA
9. Baron JS, Modi S. 2016. *Assessing the fleet-wide material technology and costs to lightweight vehicles*. Rep., Cent. Automot. Res.
10. Isenstadt A, German J, Bubna P, Wiseman M, Venkatakrishnan U, et al. 2016. *Lightweighting technology development and trends in U.S. passenger vehicles.* Work. Pap., Int. Counc. Clean Transp.
11. US EPA. 2016. *Light-duty vehicle CO_2 and fuel economy trends*. Rep. EPA-420-S-16-001, US EPA
12. Bullis K. 2013. Automakers shed the pounds to meet fuel efficiency standards. *MIT Technol. Rev.*, Feb. 20
13. Kunkel GA, Hovanski Y. 2016. From the lab to your driveway: aluminum tailor-welded blanks. *Weld. J.* 95(8):36–39
14. Joost WJ, Krajewski PE. 2017. Towards magnesium alloys for high-volume automotive applications. *Scr. Mater.* 128:107–12
15. Winters J. 2014. Light vehicles' lightweight future. *Mech. Eng. CIME*, Aug. 1. Accessed Nov. 28, 2017
16. Hartfield-Wünsch SE, Hall JN. 2012. Manufacturing challenges for aluminum sheet in the automotive industry. In *ICAA13*, ed. H Weiland, AD Rollett, WA Cassada, pp. 885–90. Cham, Switz.: Springer
17. Xia L. 2016. *Multiscale Structural Topology Optimization*. London: Elsevier
18. Fiedler K, Rolfe BF, De Souza T. 2017. Integrated shape and topology optimization: applications in automotive design and manufacturing. *SAE Int. J. Mater. Manuf.* 10(3):385–94
19. Keough JR, Hayrynen KL. 2000. Automotive applications of austempered ductile iron (ADI): a critical review. *SAE Trans*. 109:344–54
20. Horstemeyer MF. 2012. *Integrated Computational Materials Engineering (ICME) for Metals: Using Multi-scale Modeling to Invigorate Engineering Design with Science*. Hoboken, NJ: Wiley
21. Pollock DGB, Tresa M, Allison JE. 2008. *Integrated Computational Materials Engineering: A Transformational Discipline for Improved Competitiveness and National Security*. Washington, DC: Natl. Acad. Press
22. Allison J, Li M, Wolverton C, Su XM. 2006. Virtual aluminum castings: an industrial application of ICME. *JOM* 58(11):28–35

23. Sames WJ, List FA, Pannala S, Dehoff RR, Babu SS. 2016. The metallurgy and processing science of metal additive manufacturing. *Int. Mater. Rev.* 61(5):315–60
24. Daehn G. 2017. *Metamorphic manufacturing*. Abstract, LIFT. **https://lift.technology/pillar/novel-agile-processing/**. Accessed Nov. 30, 2017
25. Allwood JM, Utsunomiya H. 2006. A survey of flexible forming processes in Japan. *Int. J. Mach. Tools Manuf.* 46(15):1939–60
26. Allwood J, Houghton N, Jackson K. 2005. The design of an incremental sheet forming machine. *Adv. Mater. Res.* 6–8:471–78
27. Cao J, Huang Y, Reddy NV, Malhotra R, Wang Y. 2008. Incremental sheet metal forming: advances and challenges. In *Proceedings of International Conference on Technology of Plasticity (ICTP 2008)*. Gyeongju, Korea: Korean Soc. Technol. Plastic.
28. Taub AI, Babu SS. 2018. Opportunities and challenges for introducing new lightweight metals in transportation. *Int. J. Powder Metall.* 54(2):27–33
29. Taub AI, Luo AA. 2015. Advanced lightweight materials and manufacturing processes for automotive applications. *MRS Bull.* 40(12):1045–54
30. Skszek T, Conklin J, Zaluzec M, Wagner D. 2014. *Multi-material lightweight vehicles: Mach-II design*. Rep. for US Dep. Energy. **https://energy.gov/sites/prod/files/2014/07/f17/lm088_skszek_2014_o.pdf**. Accessed Dec. 1, 2017
31. Skszek T. 2015. *Demonstration project for a multi-material lightweight prototype vehicle as part of the clean energy dialogue with Canada*. Final Rep. for US Dep. Energy (award DE-EE0005574)
32. Henriksson F. 2016. *An outlook on multi material body solutions in the automotive industry: possibilities and manufacturing challenges*. Tech. Pap. 2016-01-1332, SAE
33. US Dep. Energy. 2010. *2010 annual progress report: lightweight material*. Rep., US Dep. Energy. **https://www.energy.gov/sites/prod/files/2014/03/f8/2010_lightweighting_materials.pdf**. Accessed Sept. 1, 2015
34. US EPA. 2012. *Light-duty vehicle mass reduction and cost analysis—midsize crossover utility vehicle*. Rep. EPA-420-R-12-026, US EPA. **https://nepis.epa.gov/Exe/ZyPDF.cgi/P100EWVL.PDF?Dockey=P100EWVL.PDF**
35. Gehm R. 2016. Multi-material structures move mpg upward. *Automot. Eng.* 2016(3):18–21
36. Singh H. 2012. *Mass reduction for light-duty vehicles for model years 2017–2025*. Rep. DOT HS 811 666, US Dep. Transp.
37. US EPA. 2015. *Mass reduction and cost analysis: light duty pickup model years 2020–2025*. Rep. EPA-420-R-15-006, US EPA
38. Vasalash GS. 2017. Light vehicles and how they got that way. *Automotive Design and Production*, Oct. 11. **https://www.adandp.media/articles/light-vehicles-and-how-they-got-that-way**
39. Monaghan M. 2012. Light and mighty. *Automot. Eng.* 2012(7):20–24
40. Steven A. 2015. Mixing metals. *Automot. Eng.* 2015:27–29
41. Wagner DA, Zaluzec MJ. 2015. Mixed materials drive lightweight vehicle design. *Adv. Mater. Process.* 2015(3):18–23
42. Meschut G, Janzen V, Olfermann T. 2014. Innovative and highly productive joining technologies for multi-material lightweight car body structures. *J. Mater. Eng. Perform.* 23(5):1515–23
43. Ghosh D, Pancholi L, Sathaye A. 2014. Forming a strong bond. *Automot. Eng.* 2014:24–29
44. Gould JE. 2012. Joining aluminum sheet in the automotive industry—a 30 year history. *Weld. J.* 91:23–34
45. WorldAutoSteel. 2017. *Advanced high-strength steels application guidelines version 6.0*. **https://www.worldautosteel.org/projects/advanced-high-strength-steel-application-guidelines/**. Accessed Oct. 2018
46. De Moor E, Gibbs PJ, Speer JG, Matlock DK, Schroth JG. 2010. Strategies for third-generation advanced high-strength steel development. *AIST Trans.* 7(3):133–44
47. Matlock DK, Speer JG. 2009. Third generation of AHSS: microstructure design concepts. In *Microstructure and Texture in Steels and Other Materials*, ed. A Haldar, S Suwas, D Bhattacharjee, pp. 185–205. New York: Springer

48. Matlock DK, Speer JG. 2006. Design considerations for the next generation of advanced high strength steels. In *Proceedings of the Third International Conference on Advanced Structural Steels*, ed. HC Lee, pp. 774–81. Seoul, Korea: Korean Institute of Metals and Materials
49. Olson GB. 1984. Transformation plasticity and the stability of plastic flow. In *Deformation, Processing and Structure*, ed. G Krauss, pp. 391–424. Materials Park, OH: ASM
50. Matlock DK, Speer JG, De Moor E, Gibbs PJ. 2011. TRIP steels—historical perspectives and recent developments. In *Proceedings of the 1st International Conference on High Manganese Steels, HMnS2011*. Seoul, Korea: Yonsei Univ. Press
51. De Cooman BC. 2004. Structure-properties relationship in TRIP steels containing carbide-free bainite. *Curr. Opin. Solid State Mater. Sci.* 8(3–4):285–303
52. Sugimoto K, Murata M, Song SM. 2010. Formability of A1-Nb bearing ultra high-strength TRIP-aided sheet steels with bainite ferrite and/or martensite matrix. *ISIJ Int.* 50(1):162–68
53. Rana R, De Moor E, Speer JG, Matlock DK. 2018. On the importance of adiabatic heating on deformation behavior of medium-manganese sheet steels. *JOM* 70(5):706–13
54. Lee S, De Cooman BC. 2014. Tensile behavior of intercritically annealed 10 pct Mn multi-phase steel. *Metall. Mater. Trans. A* 45(2):709–16
55. Merwin MJ. 2007. Low-carbon manganese TRIP steels. *Mater. Sci. Forum* 539–543:4327–32
56. Merwin MJ. 2007. *Hot- and cold-rolled low-carbon manganese TRIPS steels*. Tech. Pap. 2007-01-0336, SAE
57. Bhadeshia HKDH. 2010. Nanostructured bainite. *Proc. R. Soc. A* 466(2113):3–18
58. Speer JG, De Moor E, Findley KO, Matlock DK, De Cooman BC, Edmonds DV. 2011. Analysis of microstructure evolution in quenching and partitioning automotive sheet steel. *Metall. Mater. Trans. A* 42(12):3591–601
59. Wang L, Speer JG. 2013. Quenching and partitioning steel heat treatment. In *ASM Handbook, Volume 4A: Steel Heat Treating Fundamentals and Processes*, ed. GE Dossett, J Totten, pp. 317–26. Materials Park, OH: ASM Int.
60. Sugimoto K, Iida T, Sakaguchi J, Kashima T. 2000. Retained austenite characteristics and tensile properties in a TRIP type bainitic sheet steel. *ISIJ Int.* 40(9):902–8
61. Sugimoto K, Tsunezawa M, Hojo T, Ikeda S. 2004. Ductility of 0.1-0.6C-1.5Si-1.5Mn ultra high-strength TRIP-aided sheet steels with bainitic ferrite matrix. *ISIJ Int.* 44(9):1608–14
62. Speer JG, Matlock DK, De Cooman BC, Schroth JG. 2003. Carbon partitioning into austenite after martensite transformation. *Acta Mater.* 51(9):2611–22
63. Matlock DK, Bräutigam VE, Speer JG. 2003. Application of the quenching and partitioning (Q&P) process to a medium-carbon, high-Si microalloyed bar steel. *Mater. Sci. Forum* 426–432(1):1089–94
64. Pierce DT, Coughlin DR, Williamson DL, Clarke KD, Clarke AJ, et al. 2015. Characterization of transition carbides in quench and partitioned steel microstructures by Mössbauer spectroscopy and complementary techniques. *Acta Mater.* 90:417–30
65. Speer JG, Striecher AM, Matlock DK, Rizzo F, Krauss G. 2003. Quenching and partitioning a fundamentally new process to create high strength TRIP sheet microstructures. In *Austenite Deformation and Decomposition*, ed. EB Damm, MJ Merwin, pp. 502–22. Warrendale, PA: ISS/TMS
66. Kahkonen MJ, De Moor E, Speer JG, Thomas GA. 2015. Carbon and manganese effects on quenching and partitioning response of CMnSi-steels. *SAE Int. J. Mater. Manuf.* 8(2):419–24
67. Wang L, Zhong Y, Feng W, Jin X, Speer JG. 2013. Industrial application of Q&P sheet steels. In *Proceedings of the International Symposium on New Developments in Advanced High-Strength Steels*, ed. E De Moor, HJ Jun, JG Speer, MJ Merwin, pp. 141–51. Warrendale, PA: AIST
68. Gibbs PJ, De Moor E, Merwin MJ, Clausen N, Speer JG, Matlock DK. 2011. Austenite stability effects on tensile behavior of manganese-enriched-austenite transformation-induced plasticity steel. *Metall. Mater. Trans. A* 42(12):3691–702
69. De Moor E, Matlock DK, Speer JG, Merwin MJ. 2011. Austenite stabilization through manganese enrichment. *Scr. Mater.* 64:185–88
70. Zhang Y, Wang L, Findley KO, Speer JG. 2017. Influence of temperature and grain size on austenite stability in medium manganese steels. *Metall. Mater. Trans. A* 48:2140–49

71. Rana R, Lahaye C, Ray RK. 2014. Overview of lightweight ferrous materials: strategies and promises. *JOM* 66(9):1734–46
72. Ghanbari ZN, Speer JG. 2016. Elevated- and room-temperature mechanical behaviour of Zn-coated steel sheet for hot stamping. *AST Trans*. 13(4):170–77
73. Matlock DK, Speer JG. 2009. Microalloying concepts and application in long products. *Mater. Sci. Technol.* 25:1118–25
74. Thompson RE, Matlock DK, Speer JG. 2007. The fatigue performance of high temperature vacuum carburized Nb modified 8620 steel. *SAE Trans. J. Mater. Manuf.* 116(5):392–407
75. Darragh CV. 2002. Engineered gear steels: a review. *Gear Technol*. Nov.–Dec.:33–40
76. Gynther D. 2018. *Ultrapremium*^{TM} *and endurance steels*. Presented at Great Designs in Steel, Livonia, MI. **https://www.autosteel.org/-/media/files/autosteel/great-designs-in-steel/gdis-2018/track-2---gynther---timkensteel.ashx**. Accessed July 2018
77. Findley KO, Cryderman RL, Nissan AB, Matlock DK. 2013. The effects of inclusions on fatigue performance of steel alloys. *AIST Trans*. 10(6):234–44
78. Jhaveri K, Lewis GM, Sullivan JL, Keoleian GA. 2018. Life cycle assessment of thin-wall ductile cast iron for automotive lightweighting applications. *Sustain. Mater. Technol.* 15:1–8
79. Labrecque C, Gagné M, Javaid A, Sahoo M. 2003. Production and properties of thin-wall ductile iron castings. *Int. J. Cast Met. Res.* 16:313–17
80. Borrajo JM, Martínez RA, Boeri RE, Sikora JA. 2002. Shape and count of free graphite particles in thin wall ductile iron castings. *ISIJ Int*. 42(3):257–63
81. Fraś E, Górny M, Lopez H. 2014. Thin wall ductile iron castings as substitutes for aluminum alloy castings. *Arch. Metall. Mater.* 59(2):459–65
82. Stefanescu DM, Dix LP, Ruxanda RE, Corbitt-Coburn C, Piwonka TS. 2002. Tensile properties of thin-wall ductile iron. *AFS Trans*. 2(178):1149–61
83. Górny M, Tyrała E. 2013. Effect of cooling rate on microstructure and mechanical properties of thin-walled ductile iron castings. *J. Mater. Eng. Perform.* 22(1):300–5
84. Krajewski P, Sachdev A, Luo A, Carsley J, Schroth J. 2009. Automotive aluminum and magnesium: innovation and opportunities. *Light Met. Age* 67(5):6–13
85. Healey JR. 2014. 2015 Ford F-150 makes radical jump to aluminum body. *USA Today*, Jan. 13. **https://www.usatoday.com/story/money/cars/2014/01/13/redesigned-2015-ford-f-series-pickup-f-150-aluminum/4421041/**
86. Ducker Worldwide. 2017. *Aluminum content in North American light vehicles 2016 to 2028: summary report*. Rep. for DriveAluminum
87. Krajewski PE, Schroth JG. 2007. Overview of quick plastic forming technology. *Mater. Sci. Forum* 3:551–52
88. Carter JT, Krajewski PE, Verma R. 2008. The hot blow forming of AZ31 Mg sheet: formability assessment and application development. *JOM* 60:77
89. Shehata F, Painter MJ, Pearce R. 1978. Warm forming of aluminium/magnesium alloy sheet. *J. Mech. Work. Technol.* 2:279–90
90. Ayres RA. 1977. Enhanced ductility in an aluminum–4 Pct magnesium alloy at elevated temperature. *Metall. Trans. A* 8:487–92
91. 1978. Warmed-up aluminum could beat steel to the draw. *Mater. Eng.* 88:52–54
92. Luo AK, Sachdev AA. 2007. Development of light metals automotive structural subsystems. In *Proceedings of the Light Metals Technology Conference*. Ottawa, Can.: Nat. Resour. Can.
93. Luo AA, Fu PH, Yu YD, Jiang HY, Peng LM, et al. 2008. Vacuum-assisted high pressure die casting of AZ91 magnesium alloy. *North Am. Die Cast. Assoc. Trans.* 2008:T08–83
94. Brown Z, Szymanowski B, Musser M, Saha D, Seaver S. 2009. Development of super-vacuum die casting process for magnesium alloys. *North Am. Die Cast. Assoc. Trans.*
95. Brown Z, Szymanowski B, Musser M, Saha D, Seaver S. 2007. *Manufacturing of thin wall structural automotive components through high vacuum die casting technology*. Presented at International Die Casting Congress and Exposition, Houston, TX, May 15–18

96. Casarotto F, Franke AJ, Franke R. 2012. High-pressure die cast (HPDC) aluminum alloys for automotive applications. In *Advanced Materials in Automotive Engineering*, ed. J Rowe, pp. 109–49. Sawston, UK: Woodhead
97. Apelian D. 2009. *Aluminum Cast Alloys: Enabling Tools for Improved Performance*. Wheeling, IL: N. Am. Die Cast. Assoc.
98. Taylor JA. 2012. Iron-containing intermetallic phases in Al-Si based casting alloys. *Proc. Mater. Sci.* 1:19–33
99. Dinnis CM, Taylor JA, Dahle AK. 2006. Interactions between iron, manganese, and the Al-Si eutectic in hypoeutectic Al-Si alloys. *Metall. Mater. Trans. A* 37:3283–91
100. Ceschini L, Boromei I, Morri A, Seifeddine S, Svensson IJ. 2009. Microstructure, tensile and fatigue properties of the Al–10% Si–2% Cu alloy with different Fe and Mn content cast under controlled conditions. *J. Mater. Proc. Technol.* 209:5669–79
101. Cinkilic E, Sun W, Klarner AD, Luo AA. 2015. *Use of CALPHAD modeling in controlling microstructure of cast aluminum alloys*. Pap. 15-044, Am. Foundry Soc.
102. Klarner AD, et al. 2017. A new fluidity die for castability evaluation of high pressure die cast alloys. *Trans. North Am. Die Cast. Assoc.* T17–101
103. Luo AA. 2013. Application of computational thermodynamics and CALPHAD in magnesium alloy development. In *Proc. 2nd World Congr. Integr. Comput. Mater. Eng.*, ed. M Li, C Campbell, K Thornton, E Holm, P Gumbsch, pp. 3–8. Warrendale, PA: TMS
104. Am. Chem. Counc. 2018. *Plastics and polymer composites in light vehicles*. Rep., Am. Chem. Counc.
105. Institute for Advanced Composites Manufacturing Innovation (IACMI). 2017. *Phase two roadmap*. Feb. 2017. **http://www.iacmi.org**
106. Vaidya U. 2017. Advanced composite materials and manufacturing in vehicles, wind and compressed gas storage. *Text. World*, Mar. 21
107. Cedric B. 2016. *New developments for mass production of epoxy automotive composites*. Presented at Global Automotive Lightweight Materials Conference, Detroit. Accessed Aug. 2018
108. Gardiner G. 2015. HP-RTM on the rise. *Compos. World*, Apr. 14
109. Gardiner G. 2016. Wet compression molding. *Compos. World*, Jan. 2
110. Rocky Mt. Inst. 2013. *Kickstarting the widespread adoption of automotive carbon fiber composites: key findings and next steps*. Rep., Rocky Mt. Inst.
111. Thattaiparthasarathy K, Pillay S, Bansal D, Ning H, Vaidya U. 2013. Processing and characterization of continuous fibre tapes co-moulded with long fibre reinforced thermoplastics. *Polym. Polym. Compos.* 21(8):483–94
112. Emerson D, Grauer D, Hang B, Reif M, Henning F, et al. 2012. *Using unidirectional glass tapes to improve impact performance of thermoplastic composites in automotive applications*. Presented at Soc. Plast. Eng. Automot. Compos. Conf. Exhib., Troy, MI, Sept. 11–13
113. LayStitch Technology. 2018. *Print technology*. **http://www.laystitch.com/Technology.html**. Accessed Aug. 2018
114. Behrens BA, Raatz A, Hubner S, Bonk C, Bohne F, et al. 2017. Automated stamp forming of continuous fiber reinforced thermoplastics for complex shell geometries. *Proc. CIRP* 66:113–18
115. Vaidya UK. 2010. *Composites for Automotive*, *Truck and Mass Transit*. Lancaster, PA: DES*tech*
116. Thattaiparthasarathy KB. 2008. Process simulation, design and manufacturing of a long fiber thermoplastic composite for mass transit application. *Composites A Appl. Sci. Manuf.* 39(9):1512–21
117. Thomason JL, Vlug MA. 1996. Influence of fiber length and concentration on the properties of glass fibre–reinforced polypropylene. 1. Tensile and flexural modulus. *Composites A Appl. Sci. Manuf.* 27(6):477–84
118. IDI Compos. 2018. *Structural thermoset composites*. **http://www.idicomposites.com/technology-stc.php**
119. Cabrera-Rios M, Castro JM. 2006. An economical way of using carbon fibers in sheet molding compound compression molding for automotive applications. *Polym. Compos.* 27(6):718–22
120. Carberry W. 2008. Airplane recycling efforts benefit Boeing operators. *AERO*, Quart. 4. **http://www.boeing.com/commercial/aeromagazine/articles/qtr_4_08/pdfs/AERO_Q408_article02.pdf**

121. IACMI. 2016. *Pioneering partnerships announced for composite recycling*. News Release, IACMI. **http://iacmi.org/2016/07/01/pioneering-partnerships-announced-composite-recycling/**. Accessed Aug. 1
122. Janney M, Ledger J, Vaidya U. 2012. *Long fiber thermoplastic composites from recycled carbon fiber*. Presented at ISTC, 44th, Charleston, SC, Oct. 22–25
123. Janney M, Vaidya U, Sutton R, Ning H. 2014. *Re-grind study of PPS-based long fiber thermoplastic composites*. Presented at SAMPE, Seattle
124. Okine RK, Edison DH, Little NK. 1990. Properties and formability of an aligned discontinuous fiber thermoplastic composite sheet. *J. Reinf. Plast. Compos.* 9(1):70–90
125. Sloan J, ed. 2016. Composites recycling becomes a necessity. *Compos. World*, May 16. **https://www.compositesworld.com/articles/composites-recycling-becomes-a-necessity**
126. Blackman B, Kinloch A, Watts J. 1994. The plasma treatment of thermoplastic fibre composites for adhesive bonding. *Composites* 25(5):332–41
127. Brosius D, Armstrong K. 2017. *IACMI baseline cost and energy metrics*. Presentation, Mar.
128. Das S, Armstrong K. 2018. *FRPC energy use estimation tool*. **https://ornlenergyestimatortools.shinyapps.io/frpc-energy-estimator2/**
129. USDRIVE. 2015. *Materials technical team roadmap*. Rep. **https://www.energy.gov/.../MTT%20Roadmap%20UPDATE%20Apprvd%2003-11-1**
130. Baldan A. 2004. Adhesively-bonded joints and repairs in metallic alloys, polymers and composite materials: adhesives, adhesion theories and surface pretreatment. *J. Mater. Sci.* 39(1):1–49